© 2016. Published by The Company of Biologists Ltd | Development (2016) 143, 3002-3011 doi:10.1242/dev.133280

RESEARCH ARTICLE

Novel functions for *Dorsocross* in epithelial morphogenesis in the beetle *Tribolium castaneum*

Thorsten Horn and Kristen A. Panfilio*

ABSTRACT

Epithelial morphogenesis, the progressive restructuring of tissue sheets, is fundamental to embryogenesis. In insects, not only embryonic tissues but also extraembryonic (EE) epithelia play a crucial role in shaping the embryo. In *Drosophila*, the T-box transcription factor Dorsocross (Doc) is essential for EE tissue maintenance and therefore embryo survival. However, *Drosophila* possesses a single amnioserosa, whereas most insects have a distinct amnion and serosa. How does this derived situation compare with Doc function in the ancestral context of two EE epithelia? Here, we investigate the Doc orthologue in the red flour beetle, *Tribolium castaneum*, which is an excellent model for EE tissue complement and for functional, fluorescent live imaging approaches. Surprisingly, we find that *Tc-Doc* controls all major events in *Tribolium* EE morphogenesis without affecting EE tissue specification or maintenance. These macroevolutionary changes in function between *Tribolium* and *Drosophila* are accompanied by regulatory network changes, where BMP signaling and possibly the transcription factor Hindsight are downstream mediators. We propose that the ancestral role of *Doc* was to control morphogenesis and discuss how Tc-Doc could provide spatial precision for remodeling the amnion-serosa border.

KEY WORDS: *Dorsocross*, *Tribolium castaneum*, Extraembryonic development, Epithelial morphogenesis, BMP signaling

INTRODUCTION

The movement of cells and tissues is a prerequisite for morphogenesis and therefore for the development of all animals. Starting from a single cell – the zygote – different movements create the remarkable diversity of body plans and shapes between species. In the case of epithelial tissue sheets, their remodeling determines overall geometry and external form, as cells largely retain their neighbors and their polarity (St Johnston and Sanson, 2011). The final arrangement of embryonic tissues corresponds to the structures they build in the animal. In contrast, extraembryonic (EE) epithelia, generally called membranes, do not materially contribute to the embryo. However, while the EE membranes of amniotes (reptiles, birds, and mammals) become persistent compartments around the embryo until birth, insect EE membranes continue to actively reorganize and sculpt the embryo in late development (Panfilio, 2008).

Typically, insects have two extraembryonic membranes – the amnion and the serosa – which are both simple (monolayered) epithelia. In order to first provide protection to the embryo in the form of desiccation resistance (Goltsev et al., 2009; Jacobs et al., 2013; Vargas et al., 2014) and defense against pathogens (Jacobs et al., 2014), and later to leave the embryo uncovered, they perform a wide array of morphogenetic rearrangements. The degree to which EE reorganization affects the embryo ranges from small-scale effects on germ band extension and retraction in *Drosophila* (e.g. Lamka and Lipshitz, 1999) to whole-body axis inversions in hemimetabolous insects (Panfilio et al., 2006; Panfilio, 2008). Underlying these global effects are morphogenetic events including reversible cell shape changes, invagination, epiboly, and less common behaviors such as fusion, rupture and whole tissue eversion.

Interactions on the gene and cell levels may differ dramatically between species even if the overall phenotypic outcome appears to be similar (Horn et al., 2015). Hence, the high diversity of EE membrane movements in insects is ideal, not only to explore different epithelial tissue behaviors, but also to disentangle which features are conserved and which have evolved in how the process of morphogenesis is regulated. Ultimately, this will lead to a more global understanding of tissue morphogenesis across the tree of life.

Despite the importance of EE membranes in insect development, little is known about their morphogenesis because *Drosophila melanogaster*, the most advanced insect model system, only possesses a single derived EE membrane, the amnioserosa (Harden, 2002; Rafiqi et al., 2008; Schmidt-Ott, 2000). It is specified on the dorsal side of the blastoderm by the transcription factor Zerknüllt (Zen; Wakimoto et al., 1984), and it essentially remains in this position until embryonic dorsal closure. Once established, the amnioserosal anlage requires input from the U-shaped group of genes throughout development (Frank and Rushlow, 1996). One of the U-shaped genes, *Dorsocross* (*Doc*), encodes a T-box transcription factor most closely related to the Tbx6 subfamily (Hamaguchi et al., 2004; Reim et al., 2003). *Dm-Doc* has three redundant paralogues. Loss of function of all three results in a failure of amnioserosal maintenance: although specified, the tissue develops defective morphology and the cells do not survive (Reim et al., 2003). As a consequence, germ band retraction fails, causing the characteristic U-shaped phenotype of the embryo. *Dm-Doc* also has additional developmental roles in the body proper: in the heart and hindgut during embryogenesis, and later in the wing imaginal discs during metamorphosis (Hamaguchi et al., 2012; Reim and Frasch, 2005; Sui et al., 2012). Given the essential roles that *Dm-Doc* plays, we asked how this would compare to the situation in an insect species with the typical EE complement of a distinct serosa and amnion that cover the embryo.

Here, we present our investigation of Dorsocross function and EE development in the red flour beetle, *Tribolium castaneum*. *Tribolium* is a tractable experimental model that is more representative for EE development across the insects (Handel et al., 2000; Panfilio, 2008), and it possesses a single orthologue, *Tc-Doc*. As in *Drosophila*, we

Institute for Developmental Biology, University of Cologne, Zülpicher Str. 47b, Cologne 50674, Germany.

*Author for correspondence (kristen.panfilio@alum.swarthmore.edu)

T.H., 0000-0001-8181-939X; K.A.P., 0000-0002-6417-251X

Received 25 November 2015; Accepted 7 July 2016

Development (2016) 143, 3002-3011 doi:10.1242/dev.133280

find that *Tc-Doc* is essential for EE development and some of the regulatory inputs and downstream effectors are conserved, but interactions among these genetic components and their precise EE functions differ. *Tc-Doc* seems not to share any of the specific functions of its fruit fly counterpart for patterning, specification, or maintenance of different tissues, but rather plays a major role in EE morphogenetic events throughout development, including early membrane formation over the embryo and later active membrane withdrawal and dorsal closure. In particular, using parental RNAi and timed single and double gene knockdown embryonic RNAi, we demonstrate the modular nature of early EE morphogenesis, where BMP signaling via *Tc-decapentaplegic* (*Tc-dpp*) is an important downstream factor. Phenotypic data also identify the fellow U-shaped group member *Tc-hindsight* (*Tc-hnt*) as necessary for some of these events. By comparing the expression and function of *Doc* between *Tribolium* and *Drosophila*, we not only follow the evolution of the transcription factor Dorsocross but also of extraembryonic development itself.

RESULTS

Early *Tc-Doc* expression depends on Tc-Dpp in the amnion and Tc-Zen1 in the serosa

Early *Tribolium* development has been well characterized morphologically (Benton et al., 2013; Handel et al., 2000; Koelzer et al., 2014; Strobl and Stelzer, 2014). Landmark events are the differentiation of the blastoderm into serosa and germ rudiment (embryo and amnion); the flattening of the posterior pole at the primitive pit stage, marking the onset of morphogenesis; and subsequent EE fold migration to fully envelop the embryo during the serosal window (SW) closure stage (Movie 1, WT). The resulting egg topology consists of an inner amniotic cover over the embryo's ventral surface and an outer serosal cover that encloses embryo, amnion and yolk (shown schematically in Fig. 8).

Tc-Doc mRNA is first detected at the undifferentiated blastoderm stage in a dorsal anterior domain. As the blastoderm differentiates, this domain expands throughout the entire serosa (Fig. 1A,B, Fig. S1). Earlier reports described strong dorsal serosal expression only (Nunes da Fonseca et al., 2008; van der Zee et al., 2006). We additionally detect weaker expression in the ventral serosa, probably reflecting the increased sensitivity of our longer, exon-only probe (Fig. S2). Shortly after the primitive pit stage, a new domain forms in the posterior amnion, which will fold over to cover the embryo (Fig. 1C, orange arrowhead). Meanwhile, serosal expression becomes restricted to the tissue border (Fig. 1C, blue arrowhead), the domain that will later form the rim of the serosal window (Fig. 2A).

In flies, extraembryonic expression of *Doc* requires the combined activity of Dpp and Zen (Rafiqi et al., 2012; Reim et al., 2003). We therefore tested the expression of *Tc-Doc* in response to knockdown of *Tc-dpp* or *Tc-zen1*, the *Tribolium* orthologue of *Dm-zen* that is responsible for serosal specification (van der Zee et al., 2005). *Tc-dpp*^{RNAi} embryos show severe dorsal-ventral patterning defects, with a strongly ventralized fate map shift (van der Zee et al., 2006). In these embryos, *Tc-Doc* is absent from its undifferentiated blastoderm domain (Fig. 1D) and the posterior amniotic fold (Fig. 1F, orange arrowhead), which are both dorsal regions (Nunes da Fonseca et al., 2008). In contrast, expression in the (ventralized) serosa is still present and retracts to the tissue border during early morphogenesis (Fig. 1E,F, blue arrowheads; Fig. S3), similar to expression in the wild type. Conversely, after *Tc-zen1* RNAi, *Tc-Doc* expression is still present at the undifferentiated blastoderm stage (Fig. 1G), but fails to expand ventrally into what would have been the serosal domain (Fig. S1), while amniotic expression is unaffected (Fig. 1H, orange arrowheads). The functionally distinct paralogue *Tc-zen2* did not affect *Tc-Doc* expression (Fig. S4A-D). Thus, similar to the situation in *Drosophila*, in *Tribolium*, *Tc-zen1* and *Tc-dpp* serve as positive regulators of *Tc-Doc*, although here their activities are spatially complementary (*Tc-zen* in the serosa, *Tc-dpp* in the amnion) rather than combinatorial, reflecting differences in the number of extraembryonic tissues.

Late *Tc-Doc* expression is amniotic and mesodermal

At the serosal window stage, distinct bilateral *Tc-Doc* expression domains emerge over the posterior-lateral part of the head lobes (Fig. 2A). Fluorescent *in situ* hybridization shows that these domains encompass both inner and outer tissue layers of the SW rim

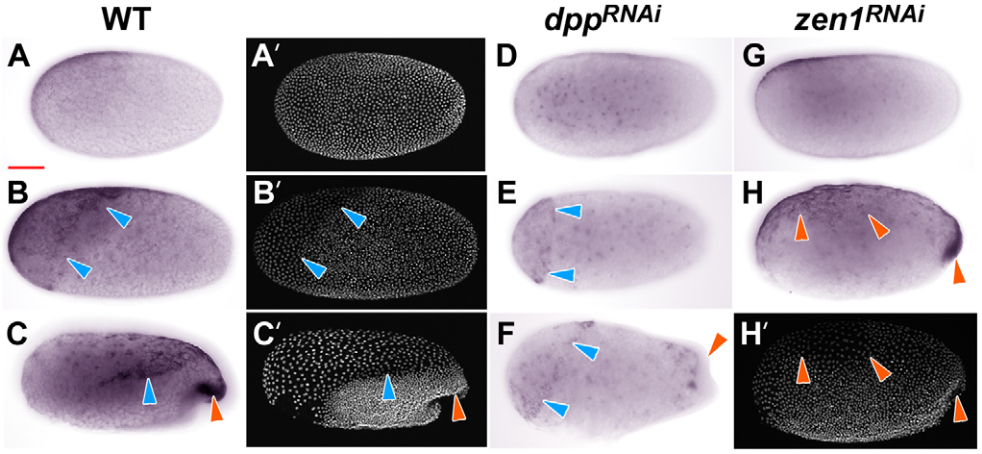

Fig. 1. Distinct serosal and amniotic domains of early *Tc-Doc* expression. (A-H) *Tc-Doc* expression assessed by *in situ* hybridization, with a nuclear counterstain (A′,B′,C′,H′). Wild-type expression starts at the undifferentiated blastoderm stage in an anterior dorsal domain (A,A′) and then expands throughout the serosa (B,B′, arrowheads). This domain then retracts to the border with the germ rudiment (C,C′, blue arrowheads) and a new domain forms in the posterior amniotic fold (C,C′, orange arrowheads). (D-F) After *Tc-dpp* RNAi, *Tc-Doc* expression is absent from the undifferentiated blastoderm (D) and the posterior amniotic fold (F, orange arrowhead), but is present in the serosa (E,F, blue arrowheads). For more details on *Tc-dpp* RNAi see Fig. S3 and Stappert et al. (2016). (G,H) After *Tc-zen1* RNAi, initial *Tc-Doc* expression is dorsal (G, also see Fig. S1), which becomes the amniotic domain flanking the embryo (H,H′, orange arrowheads). All views are lateral with anterior left and dorsal up. Red scale bar in A is 100 µm and applies to all images.

Development (2016) 143, 3002-3011 doi:10.1242/dev.133280

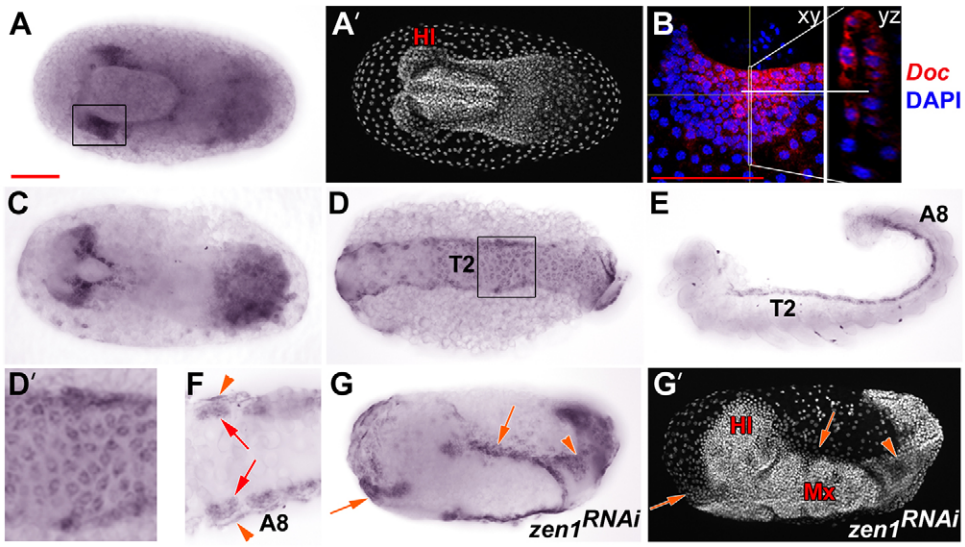

Fig. 2. Maturing extraembryonic and mesodermal *Tc-Doc* expression. (A) At the serosal window stage, *Tc-Doc* is expressed at the rim of the window, including two broader, lateral domains (boxed region). (B) Fluorescence *in situ* hybridization shows that these domains include both inner and outer layers of extraembryonic tissue (*y-z* plane). (C) *Tc-Doc* is also expressed in the amnion covering the segment addition zone at increasing levels (compare with A). (D) Amniotic expression expands throughout the tissue at the extended germ band stage (some anterior amnion has been removed in this preparation). (D′) Zoom of boxed region in D. (E,F) At the retracting germ band stage, *Tc-Doc* expression occurs in dorsal mesodermal blocks (red arrows) and persists in the amnion (orange arrowheads). (G) In germ band stage *Tc-zen1*^{RNAi} embryos, *Tc-Doc* is expressed in the part of the amnion covering the embryo ventrally (orange arrowhead) and in tissue folds flanking the embryo (orange arrows, compare with Fig. 1H). A-D and F are ventral views, E is lateral and G is ventral-lateral, with anterior left in all images. F is a flat mount view of an embryo at a similar stage to that in E. Note that the amnion has been largely removed during preparation in E and F. A′,G′ show a nuclear counterstain of the respective embryos in A and G. Scale bar: 100 µm. HI, head lobe; T2, thoracic segment 2; A8, abdominal segment 8; Mx, maxillary segment.

(Fig. 2B). Judging by nuclear size and cell tracking from live imaging (Benton et al., 2013), we suspect that *Tc-Doc* expression straddles the amnion and the serosa in this dynamically remodeling region. Expression continues in the portions of the amnion covering the posterior segment addition zone and the head lobes as the SW closes (Fig. 2C), and subsequently expands throughout the whole amnion at the extending germ band stage (Fig. 2D).

During early germ band retraction, amniotic *Tc-Doc* expression persists (Fig. 2E,F, orange arrowheads highlight lateral tissue retained in these preparations). In contrast, serosal *Tc-Doc* expression ends with the closure of the SW and was not detected subsequently (downregulation is already discernible in Fig. 2C). Consistent with this, germ band stage *Tc-Doc* amniotic expression is autonomous and still occurs in the absence of the serosa (Fig. 2G). Additionally, *Tc-Doc* expression appears in a metameric fashion within the dorsal mesoderm (Fig. 2E,F, red arrows), where the conserved mesodermal marker *Tc-Mef2* is also expressed (Cande et al., 2009) and similar to *Dm-Doc* (Reim et al., 2003). However, we could not detect *Tc-Doc* in the cardioblast mesodermal derivatives at later stages (Fig. S4E,F).

Tc-Doc knockdown is efficient but does not disrupt tissue specification or maintenance

We next used parental RNAi (pRNAi) to analyze the function of *Tc-Doc* during embryogenesis. Two non-overlapping dsRNA fragments (Table S1) resulted in qualitatively similar phenotypes. However, the second fragment achieved higher penetrance as determined by phenotypic scoring from both histological and cuticle preparations (Fig. S5A), and was therefore used for all subsequent analyses. Furthermore, we observed that these scoring methods using fixed material underestimated RNAi penetrance. With live imaging detection of transient defects (e.g. Movie 3, posture defects, see below), we obtained specific phenotypes in 93% of all embryos (Fig. 3A,B). Knockdown penetrance was stable for at least 11 days after injection (Fig. S5B), with a 67% reduction in *Tc-Doc* expression as determined by RT-qPCR (Fig. 3C, Fig. S5C). Direct detection of *Tc-Doc* transcript by *in situ* hybridization after *Tc-Doc* RNAi further showed that expression was completely absent in 59% of embryos at the differentiated blastoderm stage, with substantially reduced levels in 78% of all early embryos examined (Fig. 3C, Fig. S5D).

Despite the high RNAi efficiency, knockdown of *Tc-Doc* did not disturb specification or maintenance of the EE tissues, early mesoderm specification or embryonic segmentation (Fig. S6A-D, Movies 1,2). As *Doc* is a key component for cardiogenesis in *Drosophila* (Reim and Frasch, 2005), we also tested *Tc-Doc* function in *Tribolium* heart development, using an enhancer trap line that marks the cardioblast cell row and *in situ* hybridization against the cardioblast marker *Tc-midline* (Koelzer et al., 2014). However, no obvious defects in heart development could be detected (Fig. S6E,F, Movie 2; see Discussion), consistent with the absence of *Tc-Doc* expression from this domain (Fig. S4E).

Rather than the EE maintenance defects known from *Drosophila*, in *Tribolium*, we found several temporally distinct defects linked to the morphogenetic movements of the extraembryonic tissues (Fig. 3B).

Early *Tc-Doc*^{RNAi} phenotype: impaired closure of the serosal window

SW closure is the first major EE rearrangement. Both the serosa and the amnion must undergo intra-tissue fusion and inter-tissue detachment in order to create complete, distinct EE covers (Fig. 8D-F, schematic). While the amnion then extends with the embryo, the serosa remains largely static under the eggshell, to which it becomes attached through its secreted cuticle (Hilbrant et al., 2016; Jacobs et al., 2013).

Development (2016) 143, 3002-3011 doi:10.1242/dev.133280

After *Tc-Doc* RNAi, serosal window closure often does not occur (Fig. 3B, 49%, n=108). Typically, the posterior amniotic fold slows down and stops moving anteriorly (Movie 1). As a consequence, the embryo remains tethered to the serosa via the amnion, anchoring the head at the anterior ventral position where the SW usually closes (Fig. 4A,B, Movie 1). This physical constraint causes diverse posture defects during germ band extension as the body twists and curls, occasionally with the gnathal segments protruding through the open SW (Fig. 4C). Remarkably, embryos can – at least partially – recover from many of these posture defects during germ band retraction.

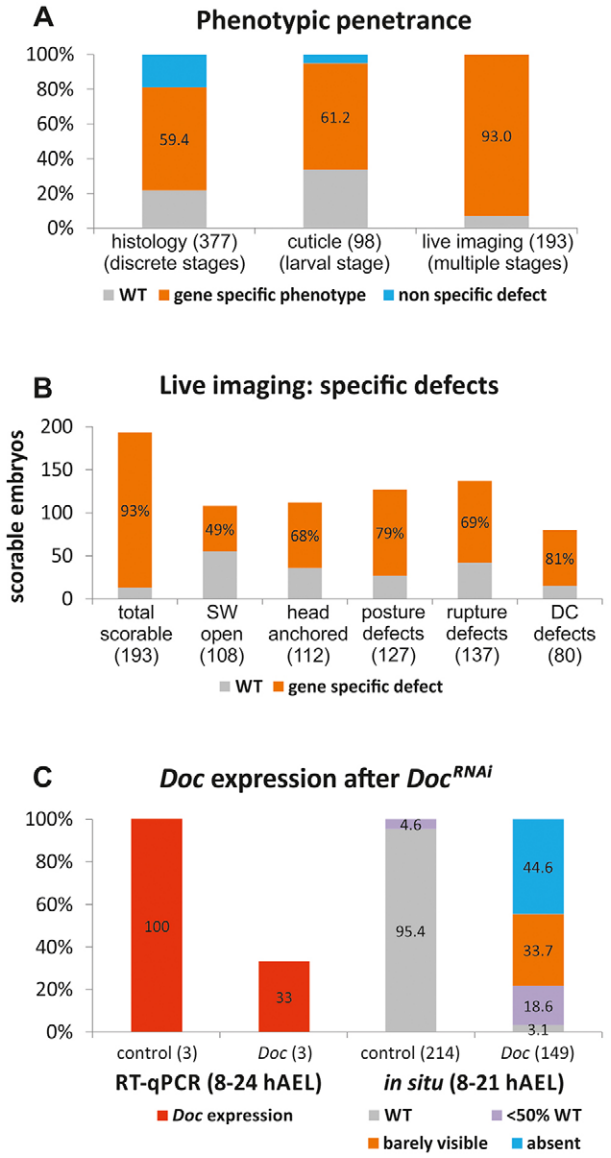

Fig. 3. Efficiency of *Tc-Doc*^{RNAi} knockdown assayed by phenotype and expression levels. (A) Phenotypic penetrance scored by embryonic histology, larval cuticle preparation and live imaging. Note that the first two scoring methods only assess discrete developmental stages, whereas live imaging spans multiple developmental stages and can detect transient defects. (B) Phenotypic scoring of five movie sessions from three RNAi experiments, with a total of 193 scorable embryos. As a result of time-lapse duration and orientation towards the camera, not all embryos could be scored for all defects. Note that all embryos with an open SW also showed an anchored head, but not vice versa. Rupture defects include all cases of a persistently open SW and/or ectopic rupture, whereas DC defects encompass EE withdrawal and dorsal closure stages. (C) *Tc-Doc* expression is substantially reduced after *Tc-Doc* RNAi, as assayed by both RT-qPCR and *in situ* hybridization. For further details on *Tc-Doc*^{RNAi} penetrance and persistence, expression scoring and specific rupture defects see Fig. S5. Data were collected from seven independent pRNAi experiments, where adult females were injected with approximately 0.3 µg dsRNA, except for the *in situ* assay where female pupae were injected with 0.12 µg dsRNA because of injection volume restrictions. Sample sizes are given in parentheses. hAEL, hours after egg lay; SW, serosal window; DC, dorsal closure.

Mid-development *Tc-Doc*^{RNAi} phenotype: impaired extension of the posterior germ band

To test whether the germ band posture defects are exclusively secondary effects of the head being anchored at a ventral position, we used embryonic RNAi (eRNAi) to circumvent the early SW defect (see Fig. S7 for an overview on eRNAi timing). When injected at 11.4-12.4 h after egg lay (hAEL), none of the embryos showed a defect in SW closure or the associated head anchoring phenotype. However, many embryos (15 of 32) still exhibited a transiently curled abdomen. Abdominal extension itself seems normal but lacks guidance over the posterior pole of the egg (Fig. 4D, Movie 3). This shows that *Tc-Doc* is necessary for proper extension of the abdomen independent of the serosal window defect.

Tc-Doc is upstream of specific *Tc-decapentaplegic* and *Tc-iroquois* domains

We next inspected the *Tribolium* orthologues of several developmental genes associated with *Doc* or involved in EE development in *Drosophila* (Hamaguchi et al., 2004, 2012; Reim et al., 2003; Reim and Frasch, 2005; Sui et al., 2012). For example, *Drosophila Doc* has a morphogenetic role in the wing imaginal disc, where it regulates extracellular matrix remodeling through Matrix metalloproteinase 2 (Mmp2, Sui et al., 2012). However, we found that parental RNAi against the *Tribolium* orthologue was lethal prior to the SW stage, in contrast to results from Knorr et al. (2009) (Fig. S8). RT-qPCR analysis also showed no change in the low levels of *Tc-Mmp2* during early embryogenesis after *Tc-Doc* RNAi (Fig. S5C). Meanwhile, although the EE marker genes *Tc-zen1*, *Tc-zen2* and *Tc-pannier* (van der Zee et al., 2005, 2006) were

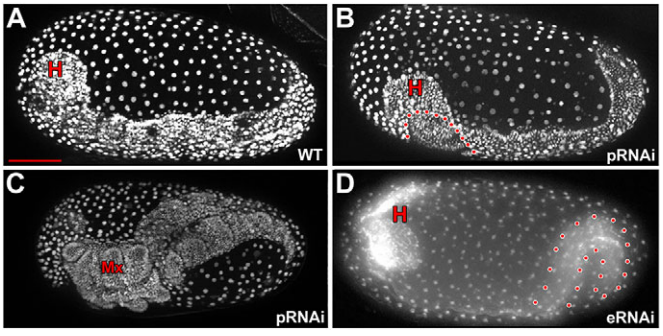

Fig. 4. *Tc-Doc* RNAi prevents serosal window closure and impairs germ band extension. (A) Wild type. (B) *Tc-Doc* parental RNAi at a comparable developmental stage to A. (C) The open SW frequently persists to later stages and is paired with a twist in the body. (D) Embryonic RNAi at about 12 hAEL bypasses the serosal window open defect, but still causes posterior embryonic posture defects. All embryos are visualized by transgenic nuclear GFP (nGFP). A and B are lateral views (see Movie 1), C is ventral-lateral and D is dorsal-lateral (see Movie 3). Red dotted outlines demarcate the border of the serosal window or the curled abdomen. Scale bar: 100 µm. H, head; Mx, maxillary segment; pRNAi, parental RNAi; eRNAi, embryonic RNAi.

Development (2016) 143, 3002-3011 doi:10.1242/dev.133280

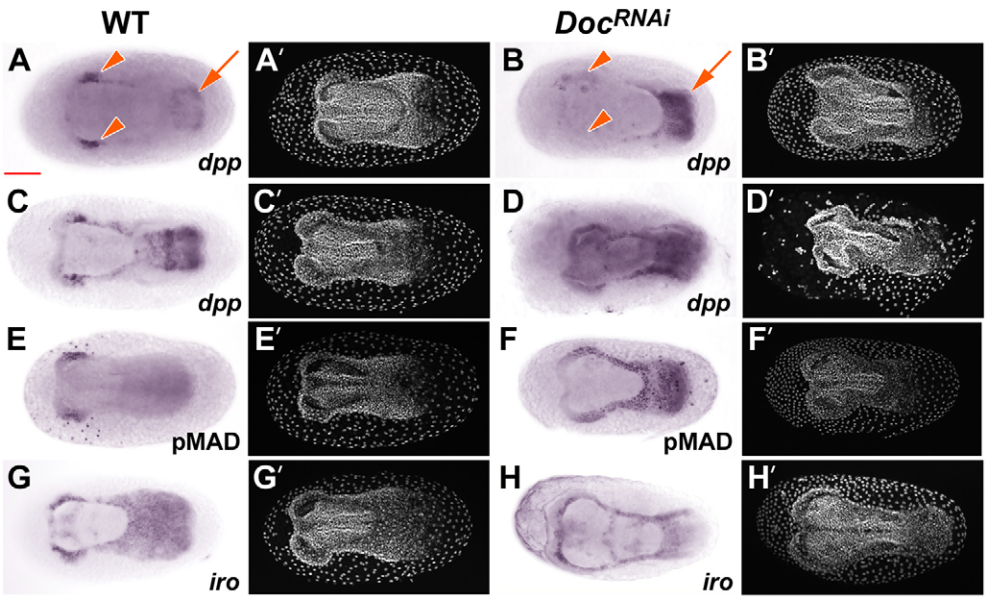

Fig. 5. Expression of *Tc-dpp*, pMAD and *Tc-iro* are altered after *Tc-Doc* RNAi. (A,C) In the wild type, *Tc-dpp* is expressed in the same bilateral domains (orange arrowheads) as *Tc-Doc* (Fig. 2A). (B,D) After *Tc-Doc* RNAi, these expression domains are absent, although *Tc-dpp* is expressed earlier in the posterior amnion (orange arrow) and more strongly throughout the late serosal window (D). (E,F) Similarly, antibody staining against the downstream effector pMAD shows a loss of the bilateral domains and an expansion of signaling throughout the serosal window and the posterior amnion. (G-H) Transcript enrichment of the amnion marker *Tc-iro* specifically in the bilateral region is also lost. All images are ventral views with anterior left. (A′-H′) Nuclear counterstains. Scale bar: 100 µm.

unaffected by *Tc-Doc* RNAi, we did find altered expression profiles for *Tc-dpp* and *Tc-iroquois* (*Tc-iro*).

Early *Tc-dpp* expression peaks in a stripe domain along the serosa/germ rudiment border (Chen et al., 2000; van der Zee et al., 2006). We found that subsequent wild-type expression of *Tc-dpp* largely resembles *Tc-Doc* expression, including increasing expression in the posterior amnion during the SW stage and expression in the lateral SW domains over the head lobes (compare Fig. 5A,C with Fig. 2A,C). After *Tc-Doc* RNAi we found two distinct changes in *Tc-dpp* expression. Firstly, the early posterior amniotic expression was much stronger (Fig. 5B,D, orange arrow). Secondly, *Tc-dpp* was initially absent in the lateral SW domains (Fig. 5B, orange arrowheads), but was then expressed throughout the whole SW at the time when it would already have closed in the wild type (Fig. 5D). We confirmed the local activity of Tc-Dpp in these domains with antibody staining against its downstream effector pMAD (Persson et al., 1998). In the wild type, strong pMAD accumulation is restricted to the lateral SW domains and adjacent regions of the serosa (Fig. 5E). In contrast, *Tc-Doc*^{RNAi} embryos showed pMAD in the posterior amnion and posterior SW, but without distinct lateral SW domains (Fig. 5F).

The earliest changes in expression of *Tc-dpp* and pMAD in response to *Tc-Doc* RNAi occur just when the *Tc-Doc*^{RNAi} phenotype first manifests. We therefore asked if loss of Dpp signaling could also affect SW closure. The profound ventralization resulting from pRNAi of *Tc-dpp* precludes SW formation (van der Zee et al., 2006). We therefore used eRNAi to avoid these early patterning defects and injected dsRNA against *Tc-dpp* at various time points (Fig. S7). Even when injecting at 7-8 hAEL, the phenotype was similar to that after pRNAi (Fig. S3). However, with injections at 11.3-12.4 hAEL, all embryos managed to close the SW (n=15), but one-fifth still showed defects in the anterior amnion, impaired head extension and general posture defects (Movie 4). This similarity to the phenotype of *Tc-Doc*^{RNAi} embryos (Movie 3), together with the altered expression profiles (Fig. 5), suggests that Tc-Dpp indeed functions downstream of Tc-Doc.

Lastly, the amnion marker *Tc-iro* (Nunes da Fonseca et al., 2008) is also expressed in the posterior amnion and the serosal window, with enrichment in the lateral SW domains (Fig. 5G). These expression domains were altered after *Tc-Doc* RNAi (Fig. 5H). However, parental *Tc-iro* RNAi did not produce any defect in closing the SW (data not shown).

Knockdown of *Tc-hindsight* resembles the *Tc-Doc*^{RNAi} phenotype

In *Drosophila*, one of the main downstream targets of *Doc* in the amnioserosa is *hindsight* (*hnt*), another member of the U-shaped group (Reim et al., 2003). We therefore tested its expression and function with respect to *Doc* in *Tribolium*. Wild-type expression of *Tc-hnt* is exclusively serosal (Fig. 6A-D) and upon *Tc-Doc* RNAi we did not detect a clear change in its expression pattern by *in situ* hybridization or its transcript levels by RT-qPCR (Fig. S5C). However, after *Tc-zen1* RNAi, *Tc-hnt* is ectopically expressed in amniotic tissue folds (Fig. 6F), which is highly reminiscent of *Tc-Doc* expression after *Tc-zen1* RNAi (Fig. 2G) and is spatially distinct from an early, *Tc-zen1*-independent terminal domain of *Tc-hnt* (Fig. 6E). In later stages, *Tc-hnt* is also expressed in an actin-rich amniotic crease in the *Tc-zen1*^{RNAi} background (Fig. 6G, arrowhead; Panfilio et al., 2013).

As pRNAi of *Tc-hnt* led to sterility, we used eRNAi to investigate its function. Although *Tc-Doc* expression examined by *in situ* hybridization was unaffected, early injections for *Tc-hnt* RNAi (7.8-8.8 hAEL, see Fig. S7) produced a similar phenotype to that of *Tc-Doc*^{RNAi} embryos: open SW, anchored head and posture defects (Fig. 6H, Movie 5, *hnt*). An embryonic double knockdown of *Tc-hnt* and *Tc-Doc* did not significantly worsen the early phenotype (Fig. 6I, Movie 5, *Doc*/*hnt*). Thus, *Tc-hnt* and *Tc-Doc* show a highly similar early RNAi phenotype despite being largely expressed in different tissues at the SW closure stage (see Discussion).

Late *Tc-Doc*^{RNAi} phenotype: ectopic extraembryonic membrane rupture and failure of dorsal closure

In the wild type, the EE membranes must actively withdraw from the embryo to facilitate dorsal closure. This begins when the amnion and the serosa rupture underneath the head when the embryo has undergone 72% of development (Koelzer et al., 2014). The membranes then pull back to the dorsal side, where the serosa forms the characteristic dorsal organ and sinks into the yolk while the amnion provides a temporary epithelial cover until the flanks of the embryo join at the dorsal midline. Having completed

Development (2016) 143, 3002-3011 doi:10.1242/dev.133280

their roles, both EE tissues then undergo apoptosis (Panfilio et al., 2013).

After *Tc-Doc* RNAi, we found that EE membrane rupture was frequently impaired (Fig. 3B, 69%, n=137). Clearly, no rupture took place when the SW was still open (Fig. S5E, 27%; Movie 2). Furthermore, rupture often occurred ectopically: either posteriorly only or from both poles (Fig. 7A,B, Fig. S5E, 42%; Movie 6). Remarkably, posterior rupture resulted in successful dorsal closure in a few cases, highlighting the high plasticity of late EE development, also seen after *Tc-zen1* RNAi (Panfilio et al., 2013). However, rupture and withdrawal are highly dynamic and require tight coordination between the two EE membranes. Consequently, the vast majority of *Tc-Doc*^{RNAi} embryos showed withdrawal defects that compromised tissue integrity, resulting in a fatal outflow of yolk (Movie 2).

As *Tc-Doc* parental RNAi efficiency waned with time after injection, we occasionally observed a failure to complete dorsal closure, despite apparently normal rupture, withdrawal and dorsal organ formation (17%, n=23, 13 days after injection). In these cases, the zippering of the flanks (Panfilio et al., 2013) initiated, but then arrested and reversed (Fig. 7C,D, Movie 7).

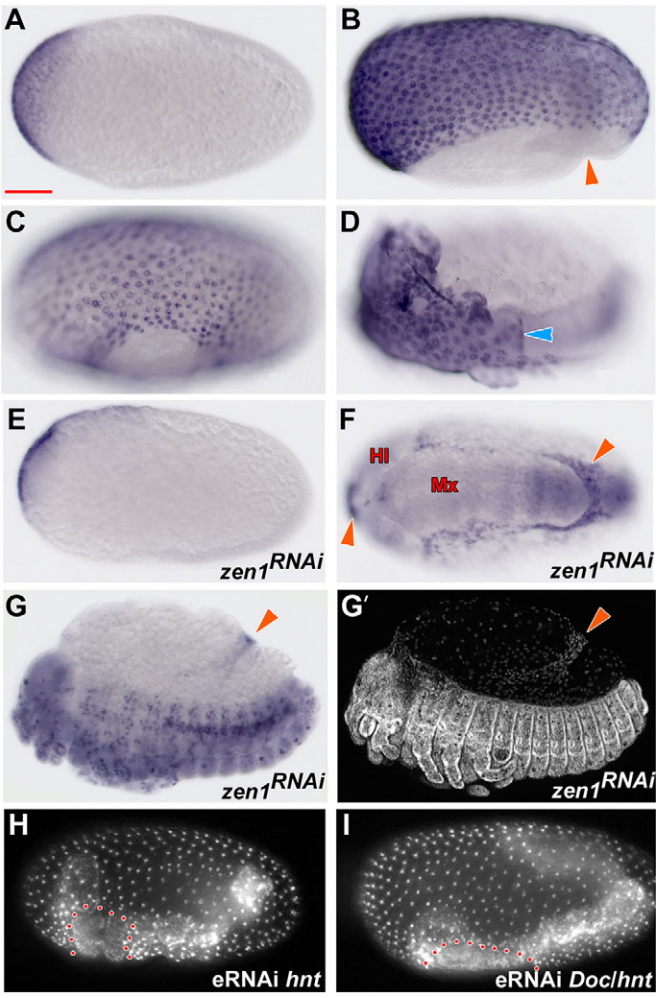

Fig. 6. *Tc-hnt* expression, regulation and function. (A-D) In the wild type, *Tc-hnt* is first expressed at the undifferentiated blastoderm stage in an anterior cap (A) and then throughout the serosa (B-D). There is no expression in the amnion (B, orange arrowhead). Note that in D the serosa (blue arrowhead) has been removed over the posterior half of the embryo, showing only minimal background levels of stain in the germ rudiment (embryo and amnion). (E-G′) After *Tc-zen1* RNAi, anterior terminal expression of *Tc-hnt* is retained but does not expand (E, differentiated blastoderm stage), whereas later, ectopic expression arises in the portions of the amnion flanking the embryo (F, arrowheads indicate anterior and posterior amniotic folds), similar to *Tc-Doc* (Fig. 2G). At the membrane withdrawal stage, ectopic *Tc-hnt* expression is also detected in the *Tc-zen1*^{RNAi} amniotic crease (G,G′, orange arrowhead; Panfilio et al., 2013), although embryonic expression throughout the peripheral nervous system, a feature conserved in *Drosophila* (Yip et al., 1997), is unaffected. (H) *Tc-hnt* RNAi results in a failure to close the serosal window (dotted outline) and impaired abdominal extension, similar to *Tc-Doc* RNAi (Fig. 4B,D). (I) Double knockdown of *Tc-Doc* and *Tc-hnt* does not enhance the phenotype. H and I are visualized by nGFP (see Movie 5). All images are lateral views except F, which is ventral. Scale bar: 100 µm. eRNAi, embryonic RNAi; HI, head lobe; Mx, maxillary segment.

DISCUSSION

Extraembryonic development in *Tribolium* is highly dynamic, with key events being serosal window closure, membrane rupture and withdrawal, and dorsal closure. These events are also the most morphogenetically challenging ones, and therefore particularly susceptible to perturbation. Nonetheless, it is striking that knockdown of *Tc-Dorsocross* interferes with all of these events without introducing any detectable defect in EE tissue specification or maintenance. Here, we first discuss the different *Tribolium* RNAi phenotypic features before we consider how *Dorsocross* and its developmental context have evolved within the insect lineage.

Tribolium Dorsocross is a key regulator of serosal window closure

Closure of the serosal window involves extensive epithelial reorganization to produce two separate EE covers over the embryo, and *Tc-Doc* plays a major role in this process. *Tc-Doc* is expressed throughout the posterior amniotic fold and at the border of the serosal window (Fig. 1C), and after *Tc-Doc* RNAi the earliest defect is the slowing down and stagnation of morphogenesis in these regions (Movie 1). We further show that Tc-Doc regulates BMP signaling in these domains, preventing early signaling in the posterior amniotic fold (Fig. 5A-F). Due to its role in dorsal-ventral patterning, we could not directly test the contribution of BMP

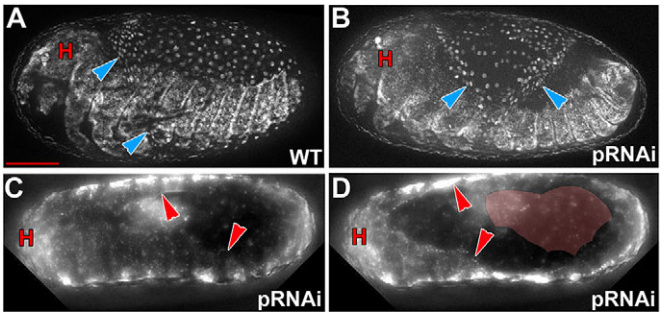

Fig. 7. Late morphogenetic defects after *Tc-Doc* RNAi. (A) In the wild type, the extraembryonic membranes rupture underneath the head and pull back to the dorsal side (blue arrowheads mark the edge of the retracting tissues, Movie 6). (B) After *Tc-Doc* RNAi, the extraembryonic tissues rupture ectopically, for example, at both poles (Movie 6). In this case, the tissues form a transient belt around the anterior abdomen, impeding EE withdrawal and embryonic dorsal closure. (C,D) Occasionally, we observed a late failure of dorsal closure alone (Movie 7). The flanks of the embryo come together and start zippering anteriorly while the posterior remains open (C, red arrowheads mark the edge of the flanks). Later, instead of joining, the flanks separate and recede ventrally (D, red shaded area indicates the limit of the flanks during maximal closure in C). All embryos are visualized by nGFP, shown laterally (A,B) or dorsally (C,D). Scale bar: 100 µm. H, head; pRNAi, parental RNAi.

Development (2016) 143, 3002-3011 doi:10.1242/dev.133280

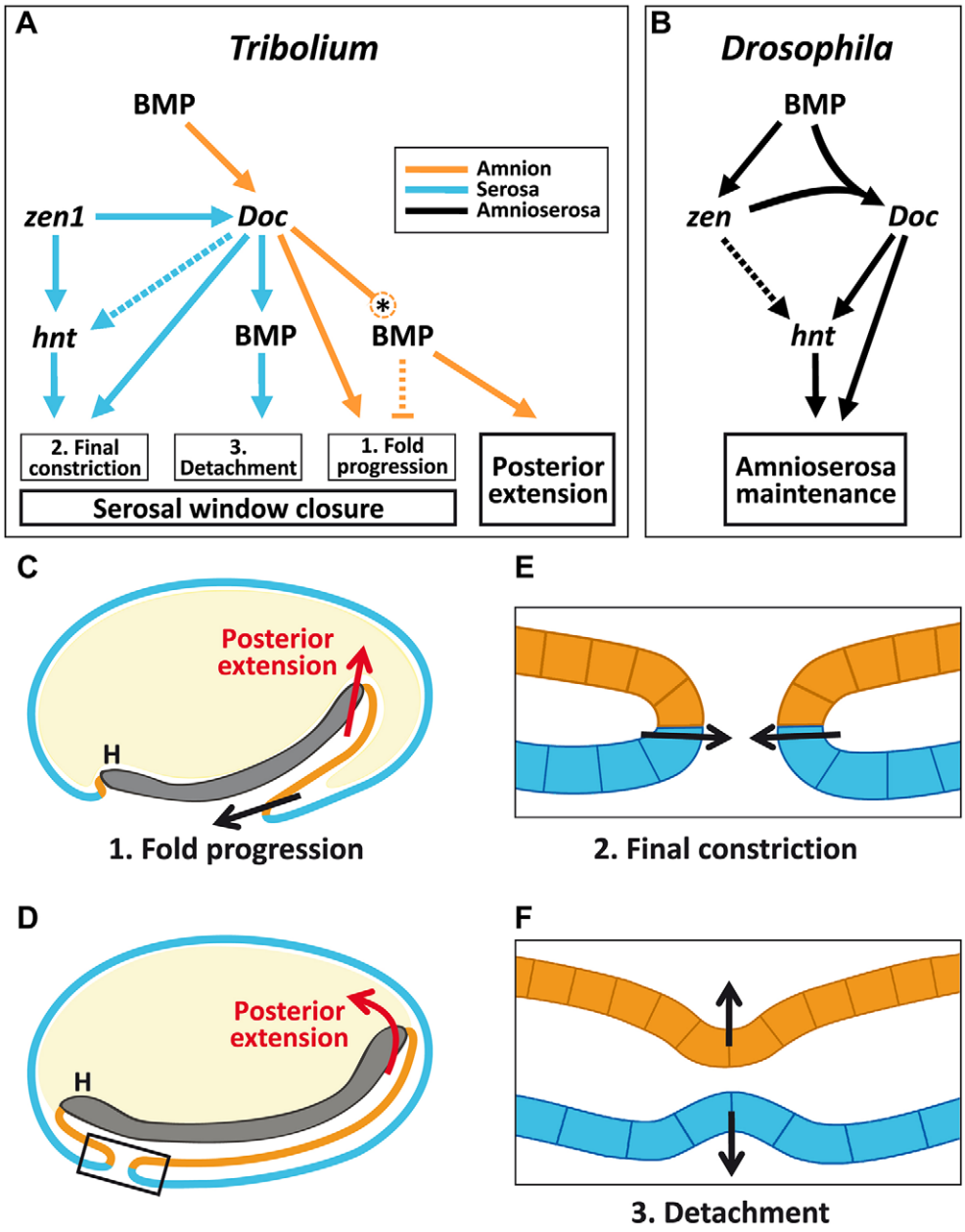

Fig. 8. Differences between gene regulatory networks driving extraembryonic development in *Tribolium* and *Drosophila*. (A) *Tribolium* gene regulatory network (GRN). BMP signaling and Tc-Zen1 activate *Tc-Doc* expression in different EE tissues (colored arrows). Serosal Tc-Doc controls final constriction of the serosal window, possibly together with Tc-Hnt, and detachment of the two extraembryonic membranes via BMP signaling. Meanwhile, amniotic *Tc-Doc* expression is necessary for posterior amniotic fold progression and posterior extension. The exact nature of BMP regulation by Tc-Doc in the amnion is complex (asterisk), as increased amniotic BMP signaling after *Tc-Doc* RNAi shows the same effect on posterior extension as BMP inhibition by *Tc-dpp* RNAi. BMP signaling downstream of Doc is highly dynamic and may involve as yet undiscovered components and feedback loops to achieve precise control of morphogenetic movements (see main text for further discussion on this point). (B) *Drosophila* GRN. BMP signaling activates *Dm-zen*, and both inputs are necessary to initiate *Dm-Doc* expression throughout the amnioserosa, where Dm-Doc, together with its downstream target Dm-Hnt, is necessary for maintenance of this tissue. (C-F) The extraembryonic morphogenetic function of *Tc-Doc* in early development involves amniotic fold progression (C, black arrow), final constriction of the serosal window (D,E), detachment of the two extraembryonic membranes (F) and posterior extension of the germ band and amnion (C,D, red arrows) as separately regulated steps. H, head.

signaling to early fold progression (Fig. 8A,C) but suggest that restriction of BMP signaling is important based on the expression patterns we observed. This is also consistent with the observation that parental *Tc-dpp* RNAi leads to greater invagination of embryonic tissue than in the wild type (van der Zee et al., 2006).

With our investigations of *Tc-hnt*, we also identified a second potential mediator of *Tc-Doc* function. It has been reported that a structure reminiscent of a supracellular actomyosin cable at the amnion-serosa border is responsible for final closure of the SW (Benton et al., 2013). The regulation of such a cable could help to explain the specific role of *Tc-Doc* and the high similarity of the *Tc-Doc* and *Tc-hnt* knockdown phenotypes (compare Movie 1 with Movie 5), despite the fact that *Tc-hnt* expression is serosal while *Tc-Doc* is predominantly amniotic at this stage. An actin cable would require input from upstream activators only in a small, defined domain at the rim of the early window, and indeed, this is the region where *Tc-hnt* and *Tc-Doc* expression coincides (compare Fig. 1C, Fig. 2A-C with Fig. 6B,C). Furthermore, simultaneous RNAi of both genes did not lead to a more severe phenotype (Fig. 6I, Movie 5), suggesting that they act in the same pathway.

Although we could not detect a role for either gene in regulating the other, subtle changes in expression at the SW rim after RNAi may have escaped our detection methods, masking a potential epistatic relationship between these genes of the U-shaped group. We suggest that *Tc-Doc* may be upstream of *Tc-hnt.* Firstly, *Drosophila Doc* is upstream of *hnt* in the amnioserosa (Reim et al., 2003). More importantly, the *Tribolium* genes have the same expression pattern after *Tc-zen1* RNAi (Fig. 2G, Fig. 6F). Despite the complete loss of the serosa, *Tc-hnt* – like *Tc-Doc* – is found in the amniotic rim. While *Tc-Doc* expression still occurs in its wild-type domain in amniotic tissue bordering the embryo, *Tc-hnt*, which would be expected to be absent in serosa-less *Tc-zen1*^{RNAi} eggs, is now present in the same domain. Assuming an interaction between the two genes, the most parsimonious explanation would be that input from *Tc-Doc* induces *Tc-hnt* ectopically in the amnion. Consistent with this hypothesis and with a specific morphogenetic

Development (2016) 143, 3002-3011 doi:10.1242/dev.133280

role, *Tc-hnt* is specifically expressed at the site of an amniotic actin cable at later stages (Fig. 6G, see also Panfilio et al., 2013). Furthermore, given that *Tc-hnt* is expressed throughout the serosa (Fig. 6B-D), it is more likely to be input from the spatially restricted *Tc-Doc* (Fig. 2A-B) that governs SW closure.

In summary, we suggest that *Tc-Doc* plays an essential role in SW closure by suppressing BMP signaling in the early amnion while activating *Tc-hnt* in the rim of the SW, thereby facilitating both fold progression and final constriction for window closure (Fig. 8A,C-E). Future elucidation of which actin binding proteins may be upregulated by Tc-Doc will clarify the link between transcriptional regulation and morphogenetic output.

Intra-tissue fusion and inter-tissue detachment are distinct extraembryonic events

Several events must occur for successful SW closure. After the posterior amniotic fold migrates anteriorly, the amnion and serosa must undergo intra-tissue fusion concomitant with inter-tissue separation (Fig. 8D-F). Although wild-type detachment of the amnion and serosa has not been documented directly, rotation of the embryo shortly after closure shows that the serosa and the amnion are free to move independently (Hilbrant et al., 2016; Koelzer et al., 2014). One frequent early defect in *Tc-Doc*^{RNAi} embryos is that the head does not extend anteriorly (Fig. 4B,C) as a result of its indirect anchoring to the serosa via the amnion. This corresponds to the site of bilateral SW expression of *Tc-Doc* and *Tc-dpp*, and we show that BMP signaling is delayed and no longer tightly localized to this domain after *Tc-Doc* RNAi (Fig. 5B,F). Furthermore, even when intra-tissue fusion occurred after late injection eRNAi of *Tc-dpp*, some embryos (20%) still exhibited mild abnormalities consistent with an amnion-serosa detachment defect (Movie 4). Hence, we distinguish detachment as a separate event (Fig. 8A,F).

The role of *Dm-Doc* in bending of the wing imaginal disc provides an explicit example of this transcription factor acting upstream to promote cell shape change via reorganization of the cellular microtubule web and a reduction of integrins and extracellular matrix components, probably through activation of *Matrix metalloproteinase 2* (Sui et al., 2012). While such remodeling events would also be important for epithelial reorganization during *Tribolium* SW closure, it remains unclear if subtle changes in *Tc-Mmp2* expression after its essential early role (Fig. S8) can contribute to the morphogenetic function of *Tc-Doc*, or whether other effectors are used here.

Tc-Doc contributes to tissue coordination throughout late morphogenesis

Even when SW closure and membrane detachment are successful, almost half of the late injected *Tc-Doc*^{eRNAi} embryos still showed an abdominal posture defect (Fig. 4D, Movie 3) that correlates with amniotic expression (Fig. 1C, Fig. 2C,D). In addition, late *Tc-dpp* eRNAi resulted in a similar abdominal phenotype (Movie 4). This suggests that regulation of BMP signaling by Tc-Doc in the amnion ensures proper extension of the posterior germ band, distinct from the earlier event of posterior fold progression (Fig. 8A, asterisk; see below). As germ band extension requires the coordination of the amnion with the embryo, extracellular signaling is likely to be important in regulating cellular rearrangements in both tissues (e.g. Nakamoto et al., 2015).

Our results further identify *Tc-Doc* as a new essential component for late EE morphogenesis. Impaired EE withdrawal after *Tc-Doc* RNAi (Fig. 7A-B) suggests that there is an underlying defect in biomechanical competence of the serosa and amnion to rupture at the endogenous anterior position (Hilbrant et al., 2016). It will be interesting to see whether *Tc-Doc* interacts with known, late EE-specific regulators such as *Tc-zen2* (van der Zee et al., 2005). Specific perturbations in the late dorsal closure event of epidermal zippering (Fig. 7C,D) also highlight a potential role of *Tc-Doc* in embryonic-extraembryonic tissue coordination.

Evolution of *Dorsocross* expression and function

We show that *Dorsocross* has multiple morphogenetic functions in *Tribolium* extraembryonic development. To understand the evolution of the functions of *Doc* within insects, we must first consider the changes in EE membrane configuration between the species we compare. In dipterans that possess two EE membranes, *Doc* is initially expressed in a dorsal domain that comprises the prospective amnion and serosa, but is later excluded from the serosa (*Anopheles*: Goltsev et al., 2007; *Megaselia*: Rafiqi et al., 2010). It has been suggested that the repression of *Doc* from the serosa is mediated by persistent *zen* expression and a switch in its role from initial activation (Rafiqi et al., 2010, 2012; Reim et al., 2003). Although *Tc-Doc* clears from the serosa during the SW stage (Fig. 2C), so too does *Tc-zen1* (Sharma et al., 2013a), whereas *Tc-zen2* does not affect *Tc-Doc* expression (Fig. S4A-D), indicating that such a repressive interaction is not conserved.

In *Drosophila*, *Dm-Doc* is necessary for the maintenance of the single amnioserosal tissue (Reim et al., 2003). Loss of function results in a defect in germ band retraction, causing the eponymous U-shaped embryonic phenotype. However, the dependence of germ band retraction on EE membranes evolved within the cyclorrhaphan fly lineage (Rafiqi et al., 2010). In *Tribolium*, the complete loss of the serosa and fundamental changes in amnion topology after *Tc-zen1* RNAi do not disturb germ band retraction (Panfilio et al., 2013; van der Zee et al., 2005). Thus, the morphogenetic context of *Tc-Doc* function is fundamentally different from that of *Dm-Doc*. In *Megaselia*, knockdown of *Ma-Doc* leads to an end-stage dorsal open phenotype, which has been attributed to a loss of amniotic cells (Rafiqi et al., 2010). This could be consistent with the maintenance function seen in the *Drosophila* amnioserosa, or with a loss of tissue integrity due to morphogenetic defects, as in *Tribolium*. Future investigations into cell and tissue rearrangements are necessary to fully address the function of *Doc* in *Megaselia*. Meanwhile, we suggest that *Doc*'s ancestral function was to direct extraembryonic morphogenesis and that this role has been lost in the dipteran lineage.

Conversely, the diverse roles of Doc in the body proper appear to be an innovation within the *Drosophila* lineage. These roles include cardioblast specification (Reim et al., 2005), dorsal-ventral patterning of the hindgut (Hamaguchi et al., 2012) and fold progression of the wing imaginal disc (Sui et al., 2012). Of these, *Tc-Doc* expression in the early mesoderm (Fig. 2E,F) would be suggestive of a role in heart development in *Tribolium* as well. However, *Tc-Doc* is not detectable in the cardioblast cells themselves (Fig. S4E), and we do not observe a clear heart-specific defect after *Tc-Doc* RNAi (Fig. S6F). Nonetheless, future work examining Doc protein expression (Reim et al., 2003) and focusing on heart development in a genetic background rescued for EE-associated postural defects that could obscure heart morphology (Reim and Frasch, 2005) could more directly address this issue.

The evolution of BMP signaling deployment in relation to Dorsocross

Consistent with the changing roles of *Doc* between *Tribolium* and *Drosophila*, we also found differences in the corresponding gene

Development (2016) 143, 3002-3011 doi:10.1242/dev.133280

regulatory networks employed in EE development (Fig. 8A-B). While strictly upstream of *Doc* in *Drosophila*, BMP signaling through the ligand Dpp plays a major role in mediating several morphogenetic functions of Doc in *Tribolium*. It seems counterintuitive that both *Tc-Doc* RNAi, which causes an early increase in BMP signaling in the posterior amniotic fold (Fig. 5B-F), and loss of BMP signaling after *Tc-dpp* RNAi result in the same abdominal extension phenotype (Movies 3,4). However, as seen for regulation of *Dm-Doc* by Dm-Zen, BMP signaling in *Tribolium* may play distinct, stage-specific roles. Alternatively, the precise dosage of BMP signaling may be important here, as has been suggested in the context of dorsal closure in *Tribolium* (Sharma et al., 2013b) and *Drosophila* (Wada et al., 2007). Indeed, similar mechanisms to control tissue sheet movements during dorsal closure may also apply to BMP's morphogenetic role in the early posterior amnion. The lack of Dpp regulation by Doc in *Drosophila* could be because *Drosophila* EE morphogenesis is highly reduced compared with *Tribolium*, eliminating the need for morphogenetic BMP signaling in the amnioserosa. Further investigation of the regulatory context and feedback loops in which BMP signaling operates (e.g. Gavin-Smyth et al., 2013), including in additional insect species, will enhance our understanding of the role of this pleiotropic pathway in epithelial remodeling.

Altogether, our results open the way for a better understanding of the diverse epithelial reorganization events observed in *Tribolium* and in animals in general. They also provide an excellent case study for investigating how transcription factors can change function during evolution, including switching from morphogenetic instruction to a tissue maintenance function, and changing expression from extraembryonic to embryonic territories to acquire novel roles in the developing embryo.

MATERIALS AND METHODS

Tribolium castaneum (Herbst) stocks

San Bernardino (SB) wild type (Brown et al., 2009), nuclear GFP (nGFP) (Sarrazin et al., 2012), and heart (G04609) and serosa (G12424) enhancer trap (Koelzer et al., 2014) lines were kept under standard culturing conditions (Brown et al., 2009) at 30°C, 40% RH. SB and nGFP were used for *in situ* hybridization, while the nGFP and enhancer trap lines were used for live imaging.

Gene-specific knockdown, histology, *in situ* hybridization and immunohistochemistry

Parental RNAi was performed as described (van der Zee et al., 2005), with double-stranded RNA (dsRNA) resuspended in double-distilled water (ddH_2O). The total mass of injected dsRNA was typically 0.3-0.4 µg per adult female and 0.1-0.15 µg per pupa. For *Tc-Doc* a total of 16 independent parental RNAi experiments were conducted, and offspring embryos were analyzed within 14 days after injection. Embryonic RNAi was typically performed with 1 µg/µl dsRNA in ddH_2O. Three rounds of injections were performed to confirm qualitatively similar phenotypes for *Tc-Doc*, *Tc-hnt* and *Tc-Doc/Tc-hnt* knockdowns: dsRNA concentration was lowered to 0.6 µg/µl for single knockdowns to achieve lower penetrance (SW open: 61% for *Tc-Doc* and 17% for *Tc-hnt*, n=23 each). Double knockdown was then performed with 0.6 µg/µl dsRNA for both genes, which restored penetrance (89%, n=28) but did not qualitatively change the phenotype. The numbers of eRNAi experiments per gene and time point are listed in Fig. S7.

Fuchsin staining ('histology', Fig. 3A, Fig. S5A) and cuticle preparation (Fig. 3A, Fig. S5B) were performed based on standard protocols (van der Zee et al., 2005; Wigand et al., 1998). *In situ* hybridization was performed as described (Koelzer et al., 2014), except for fluorescence detection, where Fast Red (Roche) was used instead of NBT-BCIP, and images were acquired with a Zeiss LSM 700 confocal microscope. All probes were tested at least three times in independent experiments with the sense probe as a negative control. Image projections were generated with Zen2 (Zeiss) or HeliconFocus 5.3 (Helicon Soft). All primer sequences for probes and dsRNA are listed in Table S1. Antibody staining was performed using standard protocols (Brown et al., 2009) with an anti-phospho-Smad1/5 rabbit antibody (Cell Signaling, 41D10, used at 1:100) and secondary detection with anti-rabbit alkaline phosphatase (Cell Signaling, 7054, used at 1:200). After *in situ* hybridization or antibody staining, embryos were mounted in Vectashield mountant containing DAPI for nuclear counterstaining (Vector Laboratories).

RT-qPCR

RNA was extracted using TRIzol reagent (Ambion) according to the manufacturer's instructions with subsequent phenol/chloroform extraction to increase purity. Total RNA quality was confirmed by agarose gel electrophoresis and spectrophotometry (NanoDrop 2000, Thermo Fisher Scientific). cDNA was synthesized using the SuperScript VILO cDNA Synthesis Kit (Invitrogen) after DNase treatment with the TURBO DNA-free Kit (Applied Biosystems). Absence of genomic DNA contamination was tested by agarose gel electrophoresis and melting curve analysis after RT-qPCR amplification with intron-spanning primers. RT-qPCR was performed on a 7500 Fast cycler (Applied Biosystems) using Fast SYBR Green Master Mix (Life Technologies). All samples were measured in three biological replicates. *Ribosomal protein S3* (*RpS3*) was chosen as a reference gene after testing eight candidate genes using NormFinder (Andersen et al., 2004). Raw data were analyzed using LinReg (Ruijter et al., 2009) and calculated in Excel (Microsoft) using the ΔΔCt method. All primer sequences for RT-qPCR are listed in Table S1.

Live imaging

Time-lapse imaging was performed as described (Panfilio et al., 2013) using Zeiss Axioplan2 and Applied Precision DeltaVision RT microscopes with post-acquisition handling in ImageJ (NIH) and Photoshop (Adobe).

Acknowledgements

We thank Nadine Frey for donation of initial *Tc-dpp*^{RNAi} materials and Maarten Hilbrant, Iris Vargas Jentzsch, Jan Seibert and Daniela Gurská for fruitful discussion, and Siegfried Roth for helpful feedback on the manuscript.

Competing interests

The authors declare no competing or financial interests.

Author contributions

T.H. and K.A.P. designed and performed research, analyzed data and wrote the paper.

Funding

This work was supported by an Emmy Noether grant from the Deutsche Forschungsgemeinschaft (German Research Foundation) [PA 2044/1-1 to K.A.P.].

Supplementary information

Supplementary information available online at
http://dev.biologists.org/lookup/doi/10.1242/dev.133280.supplemental

References

Andersen, C. L., Jensen, J. L. and Ørntoft, T. F. (2004). Normalization of real-time quantitative reverse transcription-PCR data: A model-based variance estimation approach to identify genes suited for normalization, applied to bladder and colon cancer data sets. *Cancer Res.* **64**, 5245-5250.

Benton, M. A., Akam, M. and Pavlopoulos, A. (2013). Cell and tissue dynamics during *Tribolium* embryogenesis revealed by versatile fluorescence labeling approaches. *Development* **140**, 3210-3220.

Brown, S. J., Shippy, T. D., Miller, S., Bolognesi, R., Beeman, R. W., Lorenzen, M. D., Bucher, G., Wimmer, E. A. and Klingler, M. (2009). The red flour beetle, *Tribolium castaneum* (Coleoptera): a model for studies of development and pest biology. *Cold Spring Harb. Protoc.* **2009**, pdb.emo126.

Cande, J. D., Chopra, V. S. and Levine, M. (2009). Evolving enhancer-promoter interactions within the tinman complex of the flour beetle, *Tribolium castaneum*. *Development* **136**, 3153-3160.

Chen, G., Handel, K. and Roth, S. (2000). The maternal NF-kappa B/Dorsal gradient of *Tribolium castaneum*: dynamics of early dorsoventral patterning in a short-germ beetle. *Development* **127**, 5145-5156.

Frank, L. H. and Rushlow, C. (1996). A group of genes required for maintenance of the amnioserosa tissue in *Drosophila*. *Development* **122**, 1343-1352.
Gavin-Smyth, J., Wang, Y.-C., Butler, I. and Ferguson, E. L. (2013). A genetic network conferring canalization to a bistable patterning system in *Drosophila*. *Curr. Biol.* **23**, 2296-2302.
Goltsev, Y., Fuse, N., Frasch, M., Zinzen, R. P., Lanzaro, G. and Levine, M. (2007). Evolution of the dorsal-ventral patterning network in the mosquito, *Anopheles gambiae*. *Development* **134**, 2415-2424.
Goltsev, Y., Rezende, G. L., Vranizan, K., Lanzaro, G., Valle, D. and Levine, M. (2009). Developmental and evolutionary basis for drought tolerance of the *Anopheles gambiae* embryo. *Dev. Biol.* **330**, 462-470.
Hamaguchi, T., Yabe, S., Uchiyama, H. and Murakami, R. (2004). *Drosophila* Tbx6-related gene, *Dorsocross*, mediates high levels of Dpp and Scw signal required for the development of amnioserosa and wing disc primordium. *Dev. Biol.* **265**, 355-368.
Hamaguchi, T., Takashima, S., Okamoto, A., Imaoka, M., Okumura, T. and Murakami, R. (2012). Dorsoventral patterning of the *Drosophila* hindgut is determined by interaction of genes under the control of two independent gene regulatory systems, the dorsal and terminal systems. *Mech. Dev.* **129**, 236-243.
Handel, K., Grünfelder, C. G., Roth, S. and Sander, K. (2000). *Tribolium* embryogenesis: a SEM study of cell shapes and movements from blastoderm to serosal closure. *Dev. Genes Evol.* **210**, 167-179.
Harden, N. (2002). Signaling pathways directing the movement and fusion of epithelial sheets: lessons from dorsal closure in *Drosophila*. *Differentiation* **70**, 181-203.
Hilbrant, M., Horn, T., Koelzer, S. and Panfilio, K. A. (2016). The beetle amnion and serosa functionally interact as apposed epithelia. *eLife* **5**, e13834.
Horn, T., Hilbrant, M. and Panfilio, K. A. (2015). Evolution of epithelial morphogenesis: phenotypic integration across multiple levels of biological organization. *Front. Genet.* **6**, 303.
Jacobs, C. G. C., Rezende, G. L., Lamers, G. E. M. and van der Zee, M. (2013). The extraembryonic serosa protects the insect egg against desiccation. *Proc. R. Soc. B Biol. Sci.* **280**, 20131082.
Jacobs, C. G. C., Spaink, H. P. and van der Zee, M. (2014). The extraembryonic serosa is a frontier epithelium providing the insect egg with a full-range innate immune response. *eLife* **3**, e04111.
Knorr, E., Schmidtberg, H., Vilcinskas, A. and Altincicek, B. (2009). MMPs regulate both development and immunity in the *Tribolium* model insect. *PLoS ONE* **4**, e4751.
Koelzer, S., Kölsch, Y. and Panfilio, K. A. (2014). Visualizing late insect embryogenesis: extraembryonic and mesodermal enhancer trap expression in the beetle *Tribolium castaneum*. *PLoS ONE* **9**, e103967.
Lamka, M. L. and Lipshitz, H. D. (1999). Role of the amnioserosa in germ band retraction of the *Drosophila melanogaster* embryo. *Dev. Biol.* **214**, 102-112.
Nakamoto, A., Hester, S. D., Constantinou, S. J., Blaine, W. G., Tewksbury, A. B., Matei, M. T., Nagy, L. M. and Williams, T. A. (2015). Changing cell behaviours during beetle embryogenesis correlates with slowing of segmentation. *Nat. Commun.* **6**, 6635.
Nunes da Fonseca, R., von Levetzow, C., Kalscheuer, P., Basal, A., van der Zee, M. and Roth, S. (2008). Self-regulatory circuits in dorsoventral axis formation of the short-germ beetle *Tribolium castaneum*. *Dev. Cell* **14**, 605-615.
Panfilio, K. A. (2008). Extraembryonic development in insects and the acrobatics of blastokinesis. *Dev. Biol.* **313**, 471-491.
Panfilio, K. A., Liu, P. Z., Akam, M. and Kaufman, T. C. (2006). *Oncopeltus fasciatus zen* is essential for serosal tissue function in katatrepsis. *Dev. Biol.* **292**, 226-243.
Panfilio, K. A., Oberhofer, G. and Roth, S. (2013). High plasticity in epithelial morphogenesis during insect dorsal closure. *Biol. Open* **2**, 1108-1118.
Persson, U., Izumi, H., Souchelnytskyi, S., Itoh, S., Grimsby, S., Engström, U., Heldin, C.-H., Funa, K. and ten Dijke, P. (1998). The L45 loop in type I receptors for TGF-beta family members is a critical determinant in specifying Smad isoform activation. *FEBS Lett.* **434**, 83-87.
Rafiqi, A. M., Lemke, S., Ferguson, S., Stauber, M. and Schmidt-Ott, U. (2008). Evolutionary origin of the amnioserosa in cyclorrhaphan flies correlates with spatial and temporal expression changes of *zen*. *Proc. Natl. Acad. Sci. USA* **105**, 234-239.
Rafiqi, A. M., Lemke, S. and Schmidt-Ott, U. (2010). Postgastrular *zen* expression is required to develop distinct amniotic and serosal epithelia in the scuttle fly *Megaselia*. *Dev. Biol.* **341**, 282-290.
Rafiqi, A. M., Park, C.-H., Kwan, C. W., Lemke, S. and Schmidt-Ott, U. (2012). BMP-dependent serosa and amnion specification in the scuttle fly *Megaselia abdita*. *Development* **139**, 3373-3382.
Reim, I. and Frasch, M. (2005). The *Dorsocross* T-box genes are key components of the regulatory network controlling early cardiogenesis in *Drosophila*. *Development* **132**, 4911-4925.
Reim, I., Lee, L.-H. and Frasch, M. (2003). The T-box-encoding *Dorsocross* genes function in amnioserosa development and the patterning of the dorsolateral germ band downstream of Dpp. *Development* **130**, 3187-3204.
Reim, I., Mohler, J. P. and Frasch, M. (2005). Tbx20-related genes, *mid* and *H15*, are required for *tinman* expression, proper patterning, and normal differentiation of cardioblasts in *Drosophila*. *Mech. Dev.* **122**, 1056-1069.
Ruijter, J. M., Ramakers, C., Hoogaars, W. M. H., Karlen, Y., Bakker, O., van den Hoff, M. J. B. and Moorman, A. F. M. (2009). Amplification efficiency: linking baseline and bias in the analysis of quantitative PCR data. *Nucleic Acids Res.* **37**, e45.
Sarrazin, A. F., Peel, A. D. and Averof, M. (2012). A segmentation clock with two-segment periodicity in insects. *Science* **336**, 338-341.
Schmidt-Ott, U. (2000). The amnioserosa is an apomorphic character of cyclorrhaphan flies. *Dev. Genes Evol.* **210**, 373-376.
Sharma, R., Beermann, A. and Schröder, R. (2013a). The dynamic expression of extraembryonic marker genes in the beetle *Tribolium castaneum* reveals the complexity of serosa and amnion formation in a short germ insect. *Gene Expr. Patterns* **13**, 362-371.
Sharma, R., Beermann, A. and Schröder, R. (2013b). FGF signalling controls anterior extraembryonic and embryonic fate in the beetle *Tribolium*. *Dev. Biol.* **381**, 121-133.
St Johnston, D. and Sanson, B. (2011). Epithelial polarity and morphogenesis. *Curr. Opin. Cell Biol.* **23**, 540-546.
Stappert, D., Frey, N., von Levetzow, C. and Roth, S. (2016). Genome-wide identification of *Tribolium* dorsoventral patterning genes. *Development* **143**, 2443-2454.
Strobl, F. and Stelzer, E. H. K. (2014). Non-invasive long-term fluorescence live imaging of *Tribolium castaneum* embryos. *Development* **141**, 2331-2338.
Sui, L. Y., Pflugfelder, G. O. and Shen, J. (2012). The Dorsocross T-box transcription factors promote tissue morphogenesis in the *Drosophila* wing imaginal disc. *Development* **139**, 2773-2782.
van der Zee, M., Berns, N. and Roth, S. (2005). Distinct functions of the *Tribolium zerknüllt* genes in serosa specification and dorsal closure. *Curr. Biol.* **15**, 624-636.
van der Zee, M., Stockhammer, O., von Levetzow, C., da Fonseca, R. N. and Roth, S. (2006). Sog/Chordin is required for ventral-to-dorsal Dpp/BMP transport and head formation in a short germ insect. *Proc. Natl. Acad. Sci. USA* **103**, 16307-16312.
Vargas, H. C. M., Farnesi, L. C., Martins, A. J., Valle, D. and Rezende, G. L. (2014). Serosal cuticle formation and distinct degrees of desiccation resistance in embryos of the mosquito vectors *Aedes aegypti*, *Anopheles aquasalis* and *Culex quinquefasciatus*. *J. Insect Physiol.* **62**, 54-60.
Wada, A., Kato, K., Uwo, M. F., Yonemura, S. and Hayashi, S. (2007). Specialized extraembryonic cells connect embryonic and extraembryonic epidermis in response to Dpp during dorsal closure in *Drosophila*. *Dev. Biol.* **301**, 340-349.
Wakimoto, B. T., Turner, F. R. and Kaufman, T. C. (1984). Defects in embryogenesis in mutants associated with the Antennapedia gene complex of *Drosophila melanogaster*. *Dev. Biol.* **102**, 147-172.
Wigand, B., Bucher, G. and Klingler, M. (1998). A simple whole mount technique for looking at *Tribolium* embryos. *Tribolium Info. Bull.* **38**, 281-283.
Yip, M. L. R., Lamka, M. L. and Lipshitz, H. D. (1997). Control of germ-band retraction in *Drosophila* by the zinc-finger protein HINDSIGHT. *Development* **124**, 2129-2141.

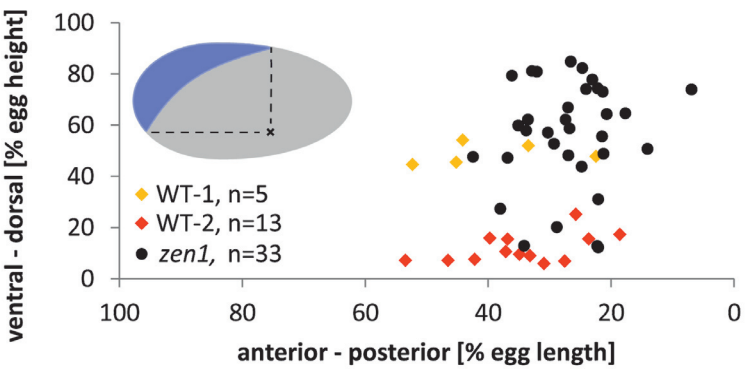

Fig. S1. Spatial analysis of early *Tc-Doc* expression in wild type and after *Tc-zen1*^{RNAi}. As *Tc-zen1*^{RNAi} embryos lack the serosa, we were not able to stage the embryos by the formation of the differentiated blastoderm. To compare early *Tc-Doc* expression between wild type and *Tc-zen1*^{RNAi} embryos we therefore recorded the maximum extension of *Tc-Doc* mRNA along the anterior-posterior and the dorsal-ventral axes. We compared wild type undifferentiated blastoderm eggs to *Tc-zen1*^{RNAi} eggs before formation of a primitive pit (therefore including stages that would be differentiated blastoderm in wild type). We found two distinct phases in wild type expression, based on the ventral extent of the expression domain (WT-1 and WT-2). WT-1 corresponds to the early stage when expression is more dorsal, while in WT-2 the expression already expands ventrally towards the edge of the presumptive serosal domain, presumably under the control of *Tc-zen1*. In contrast, *Tc-Doc* expression after *Tc-zen1*^{RNAi} remains dorsal, similar to the WT-1 category.

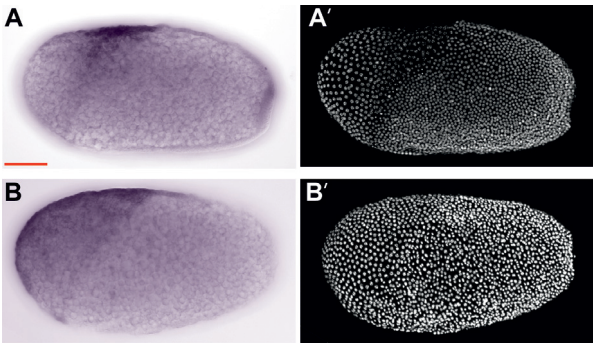

Fig. S2. *Tc-Doc* expression visualized by different *in situ* probes. *Tc-Doc* expression in the differentiated blastoderm has previously been reported to mark the dorsal part of the serosa (van der Zee et al., 2006). Here, we report expression throughout the whole serosa, albeit slightly weaker ventrally. This discrepancy can be explained by the different *in situ* probes used here and in van der Zee et al. (2006). **(A)** *Tc-Doc in situ* staining using the original plasmid to synthesize the 518-bp probe used by van der Zee, including a 60 bp intron. **(B)** *Tc-Doc in situ* using a 654-bp exon-only probe in the same experiment. Note that colorimetric detection of the probe took approximately twice the time in A as in B, arguing for a higher sensitivity of the longer probe used in this study. Primer sequence details for both probes are given in Table S1. All images are lateral views with anterior left. The red scale bar is 100 µm.

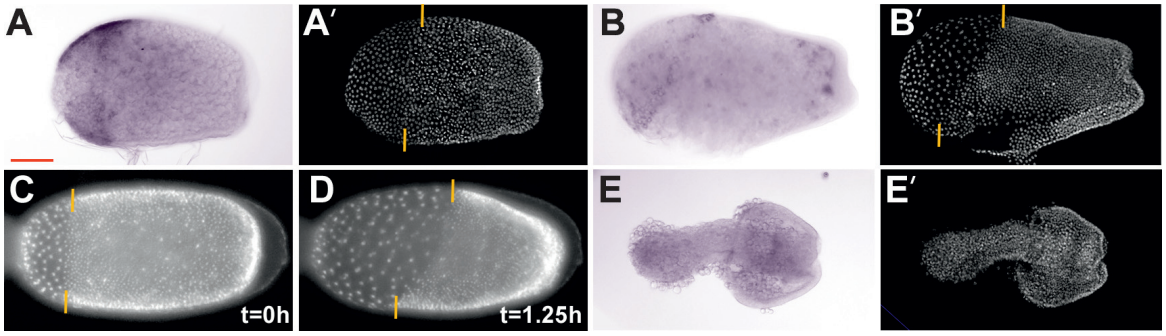

Fig. S3. *Tc-dpp*^{RNAi} embryos show a transient oblique border between the serosa and germ rudiment, with *Tc-Doc* expression only in the serosa. Knockdown of *Tc-dpp* has been reported to result in a straight border between the serosa and the germ rudiment due to complete ventralization of the blastoderm (van der Zee et al., 2006). In our experiments this was true for 85% of embryos at the differentiated blastoderm stage (n=13). However, live imaging shows that the straight border can transiently shift to an oblique conformation, reminiscent of the WT border shape, before ectopic invagination at the posterior pole occurs. This transient stage was chosen for Fig. 1F, because it shows the two key features of (1) wild type-like dynamics of *Tc-Doc* expression in retracting towards the border after the differentiated blastoderm stage and (2) the lack of *Tc-Doc* expression in the posterior amniotic fold. All images show *Tc-dpp*^{RNAi} embryos; A, B and E are *Tc-Doc in situ* staining; C and D show nuclear GFP signal from live imaging recordings. Note that serosal *Tc-Doc* expression in *Tc-dpp*^{RNAi} appears weaker than in WT (compare with main text Fig. 1). However, due to the ventralization phenotype of *Tc-dpp*^{RNAi}, serosal expression in these embryos should be compared to expression in the ventral part of WT serosa, which is weaker. In our experiments we did not find evidence for a significant difference in staining between the WT ventral serosa and the *Tc-dpp*^{RNAi} ventralized serosa. **(A)** *Tc-Doc* expression in the differentiated blastoderm stage is restricted to the serosa, which forms a straight border with the germ rudiment. **(B, reproduced from Fig. 1)** *Tc-Doc* expression retracts to the border, which is oblique during the posterior amniotic fold stage as the germ rudiment invaginates at the posterior pole. **(C, D)** Stills from live imaging of a representative *Tc-dpp*^{RNAi} embryo, showing a shift of the border from straight to oblique before posterior invagination (not shown). **(E)** During invagination, the posterior of the embryo forms a tube-like structure within the yolk while the anterior part remains at the surface of the egg (compare with van der Zee et al., 2006, supporting figures 12 and 13). Note that the serosa and yolk have been removed during fixation and there is no detectable *Tc-Doc* expression in the remaining tissues. The penetrance of this defect was 100% (n=12). All images are oriented with anterior left, and shown in lateral views where it could be determined. The orange lines demarcate the border between serosa and germ rudiment. The red scale bar is 100 μm. Embryonic material in A, B and E was a gift from Nadine Frey, from an RNAi experiment in which the expression of *Tc-dpp* itself and also of *Tc-Doc* were reduced by 60%, as determined by RT-qPCR (Stappert, D., Frey, N., von Levetzow, C. and Roth, S. (2016). Genome-wide identification of *Tribolium* dorsoventral patterning genes. *Development* 143, 2443-2454.).

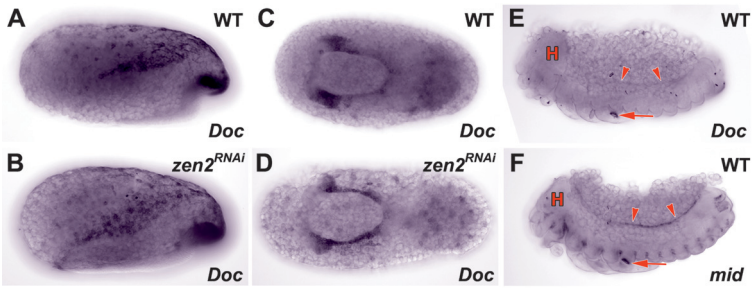

Fig. S4. *Tc-Doc* expression is not altered after *Tc-zen2*^{RNAi} and not present at the retracted germ band stage. (A, C) Wild type *Tc-Doc* expression at the posterior amniotic fold and serosal window stages (reproduced from main text Figs. 1C and 2A). **(B, D)** *Tc-Doc* expression in *Tc-zen2*^{RNAi} embryos of comparable stages is not different from wild type. **(E-F)** Although *Tc-Doc* is expressed in the early mesoderm (main text Fig. 2F), no expression could be detected at later developmental stages, including for the mesodermal derivative tissue of the cardioblast cell row (presumptive heart: red arrowheads). In contrast, the conserved cardioblast marker *Tc-mid* is expressed at this stage (F; see also Koelzer et al 2014). Note that there is unspecific staining trapped in the pleuropodia of older embryos (red arrow), a probe-independent artifact (Koelzer et al 2014). This feature was used as an internal control for the staining procedure, by allowing colorimetric staining in the pleuropodia to develop to comparable intensities for *Tc-Doc* and *Tc-mid.* All images are lateral views, except C and D, which are ventral views. Anterior is left in all images. The red scale bar is 100 µm. H, head.

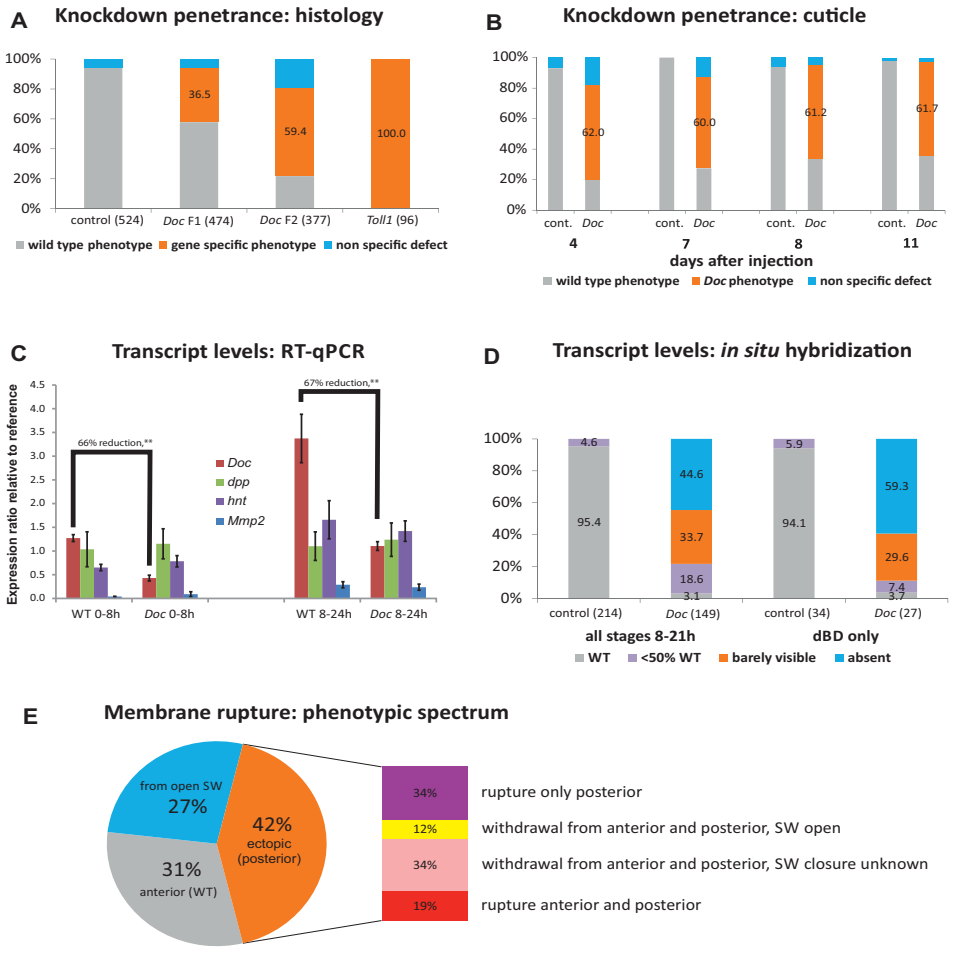

Fig. S5. Quantification of *Tc-Doc*^{RNAi} efficiency and phenotypic penetrance. (A) Comparison of two non-overlapping dsRNA fragments for *Tc-Doc*^{RNAi} (Table S1), assessed by embryonic histology with a fuchsin nuclear stain for serosal window through post-dorsal closure stages (from material collected 8-79 hAEL). Negative control embryos were from females injected with water. The positive control with *Tc-Toll1* produced 100% offspring with the *Tc-Toll1* specific phenotype (Nunes da Fonseca et al., 2008). For *Tc-Doc*, fragment F2 showed a higher penetrance than fragment F1, which was also confirmed by scoring of larval cuticle preparations from the same pRNAi experiment (*Tc-Doc* fragment F1: 33%, n= 67; *Tc-Doc* fragment F2: 67%, n= 40). Thus, fragment F2 was used for all subsequent analyses. Note that fragment F2 also generated a larger proportion of embryos with "non specific defects" than fragment F1. A fraction of this group may in fact include gene specific but milder knockdown defects, which were excluded due to the strict phenotypic scoring definitions used. Thus, the knockdown penetrance value of 59% (also shown in main text Fig. 3A) may be an underestimation. **(B)** Time course of *Tc-Doc*^{RNAi} penetrance after parental injection. The knockdown effect was stable for at least 11 days after injection, based on cuticle scoring (mean n=104, range 40-277). The data from day 8 is also shown in main text Fig. 3A. **(C)** Gene expression after *Tc-Doc*^{RNAi}, measured by RT-qPCR with the

reference gene *Tc-Ribosomal protein S3* (*Tc-RpS3*). Data are shown from three biological replicates. *Tc-Doc* mRNA levels dropped significantly (**: p<0.01 for unpaired, two-tailed *t*-test), by 66-67%, after *Tc-Doc*^{RNAi} in 0-8 and 8-24 hour old embryos, corresponding to the blastoderm stage and then to the stages from primitive pit formation through maximum germ band extension. mRNA expression of *Tc-decapentaplegic* (*Tc-dpp*), *Tc-hindsight* (*Tc-hnt*) and *Tc-Matrix metalloproteinase 2* (*Tc-Mmp2*) were not significantly changed after *Tc-Doc*^{RNAi}. **(D)** *Tc-Doc* expression examined by colorimetric *in situ* hybridization in *Tc-Doc*^{RNAi} embryos aged 8-21 hAEL. Over 94% of control embryos had strong expression that for quantification purposes was defined as "WT" levels, across all the developmental stages surveyed (left), and in particular at the key patterning stage of the differentiated blastoderm (dBD, right). A small minority showed reduced expression ("<50% of WT" strength), which may be due to experimental limitations or biological variability. In *Tc-Doc*^{RNAi}, 78% (all) and 89% (dBD only) embryos showed absent or barely visible *Tc-Doc* staining. Embryos were collected from mothers injected with dsRNA as pupae, at a concentration of approximately 0.12µg/female. **(E)** Distribution of membrane rupture defects scored by live imaging (n= 137; see main text Fig. 3B for the distribution of all defects). In 31% of the embryos, rupture occurred at the endogenous anterior position while in 27% the serosal window was not closed and membranes withdrew from there. In all cases of ectopic rupture (42%), rupture was observed from the posterior pole but varied in anterior tissue behavior (inset stacked column). Sample sizes are specified parenthetically in A and D. Abbreviations: dBD, differentiated blastoderm; SW, serosal window. Unless noted, all dsRNA was injected into adult females with approximately 0.3 µg/female.

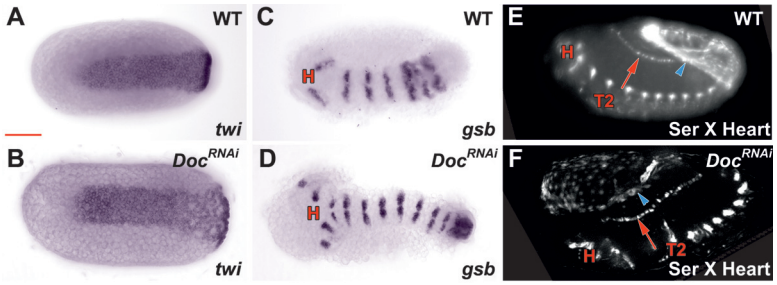

Fig. S6. Mesodermal fate, segmentation, EE tissue maintenance and cardioblast formation are unaffected by *Tc-Doc*^{RNAi}. (A-D) We used *Tc-twist* (*Tc-twi*) as a marker for mesoderm and *Tc-gooseberry* (*Tc-gsb*) as a marker of segmental development (Nunes da Fonseca et al., 2008). *in situ* hybridization in *Tc-Doc*^{RNAi} embryos did not show any defect. **(E-F)** Heterozygote cross between serosa (blue arrowhead) and cardioblast (red arrow) fluorescent marker lines (Koelzer et al., 2014). The serosal tissue persists through late EE morphogenetic rearrangements, as does the amnion (data not shown from *Tc-Doc*^{RNAi} in an amnion-GFP background, using the fluorescent transgenic line described in Hilbrant et al., 2016). Also, the cardioblast cell row was still present after *Tc-Doc*^{RNAi} (F, Movie 2). A-D are ventral views, E-F are lateral view stills from Movie 2. The red scale bar is 100 µm. H, head; Ser, serosa; T2, thoracic segment 2.

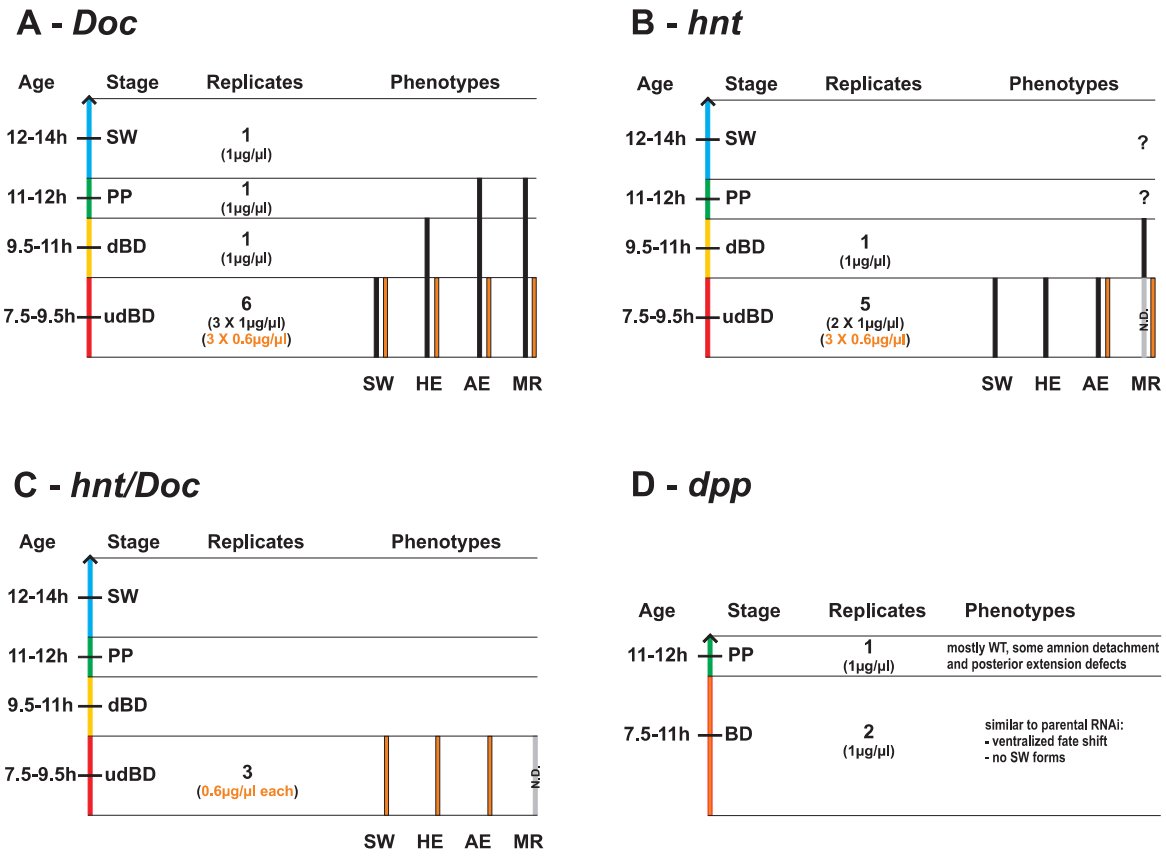

Fig. S7. Timing and obtained phenotypes from embryonic RNAi. Age and developmental stage at the time of dsRNA injection, as well as number of experimental replicates and dsRNA concentration, are indicated. Injection times are the mean of a one-hour window of egg lay. Stage abbreviations: udBD, undifferentiated blastoderm; dBD, differentiated blastoderm; PP, primitive pit stage; SW, serosal window stage. Phenotype bars indicate that at least one third of the embryos showed the corresponding phenotype after *Tc-Doc*^{RNAi} **(A)**, *Tc-hnt*^{RNAi} **(B)** and *Tc-Doc*/*Tc-hnt* double RNAi **(C)**. Phenotype bar color corresponds to dsRNA concentration. Phenotype abbreviations: SW, serosal window defect; HE, head extension defect; AE, abdominal extension defect; MR, membrane rupture defect. Developmental progression after *Tc-hnt*^{RNAi} was not monitored beyond the primitive pit stage ("?" in B), while early injected eggs in the *Tc-Doc*/ *Tc-hnt* double RNAi did not survive to rupture stage (C). **(D)** Eggs injected with *Tc-dpp* dsRNA at the blastoderm stage showed the parental RNAi phenotype (Fig. S3, see also van der Zee et al., 2006) with no serosal window forming, while eggs injected at the primitive pit stage were mostly wild type with some showing defects in anterior amnion extension and abdominal extension (see main text). Ages are shown in hours after egg lay at 30ºC. N.D., no data.

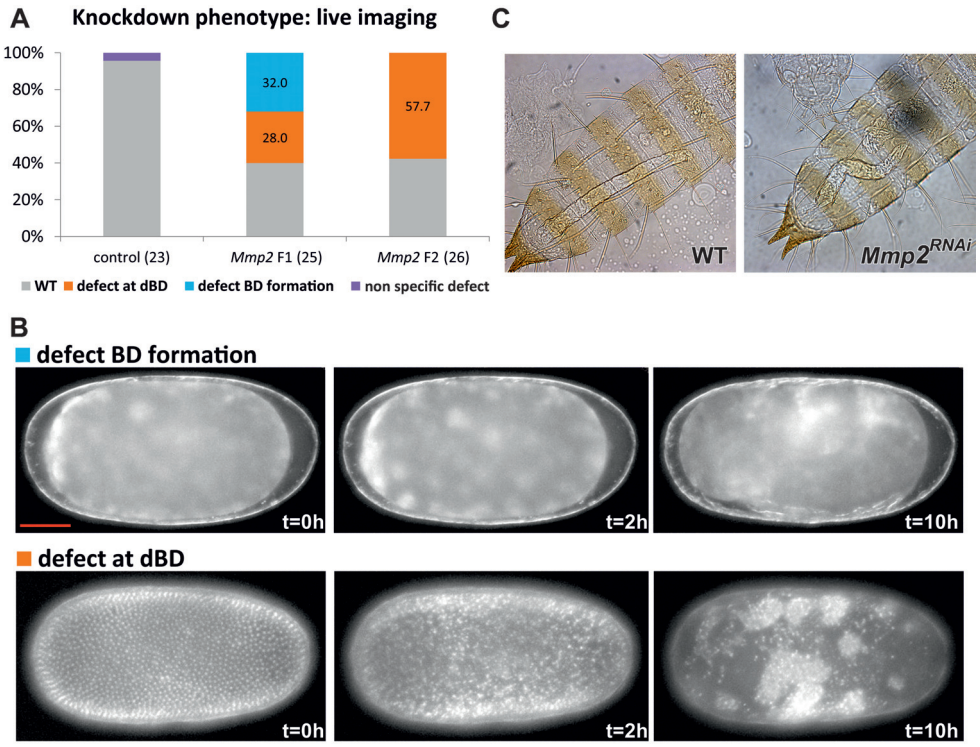

Fig. S8. Phenotype and penetrance of *Tc-Mmp2*^{RNAi}. Knockdown of *Tc-Mmp2* has previously been reported to result in only minor defects in the larval gut (Knorr et al., 2009). This is in contrast to our findings that many embryos showed severe defects at the blastoderm (BD) stage. To test for specificity, we used two non-overlapping dsRNA fragments for *Tc-Mmp2*^{RNAi} (Table S1), injecting approximately 0.2 µg dsRNA per female (the same amount Knorr et al. (2009) used). **(A)** Analysis of live imaging recordings, where 58% of the eggs failed to produce a differentiated blastoderm (dBD). However, fragment F1 seems to be slightly more severe, as nearly half of the 58% did not even form a blastoderm. **(B)** Stills from live imaging recordings showing the most severe phenotype of fragment F1, where the nuclei do not reach the surface of the egg to form a blastoderm (top), and the less severe phenotype shared by both fragments, where the undifferentiated blastoderm appears normal, but disintegrates before a differentiated blastoderm can be formed (bottom). **(C)** Consistent with the phenotype reported by Knorr et al. (2009), we observed a twisted hindgut in some of the surviving larvae. We suspect that the early lethal defects described here had escaped the authors' detection, as they inspected larval phenotypes only. It should be noted that injecting 4.8 µg dsRNA per female resulted in a penetrance of >90% for the blastoderm stage defects. BD, blastoderm; dBD, differentiated blastoderm. The red scale bar is 100 µm.

Table S1: ***Tribolium* primer sequences for RNAi, *in situ* hybridization and RT-qPCR.** All RNAi and *in situ* primers also included an adapter sequence for subsequent amplification with the T7 promoter universal primer, as described (Koelzer et al., 2014), except where marked by *. This probe was synthesized from the plasmid described by (van der Zee et al., 2006) using SP6 RNA polymerase (Roche).

RNAi			**Length**
Doc F1	forward	CCAAAAACCGTCTTTTTCCA	464 bp
	reverse	CCAGGAAGAGGCAGTAGTCG	
Doc F2	forward	TCTAAAGGCTCGCACTGGAT	469 bp
	reverse	CAGGATAAGGGCGGTAACAA	
zen1	forward	TCCCAATTTGAAAACCAAGC	688 bp
	reverse	CGTTCCACCCTTCCTGATAA	
zen2	forward	ATTACCATTCTCGGGGCTTT	374 bp
	reverse	AGTTGAGGTTTTGGGCCATT	
Mmp2 F1	forward	AAGTCCGGCTCGTCATTTC	450 bp
	reverse	GCTTGATCCTGTCCCACAAT	
Mmp2 F2	forward	CCATGCATCCCGATAAGAAG	413 bp
	reverse	GAGTCGATTTCCGGTGAAAA	
dpp	forward	AGATCGACACTGTTGCCCCTTTT	500 bp
	reverse	AGATGGTTGGTTTTGGGGTCTTG	
iro	forward	CCCGAAGTGTCGGTGTCTAC	526 bp
	reverse	TCCCGTTTGTCCTCTTCATC	
Toll1	forward	GCCGTTTCGCTCGTAACTCT	763 bp
	reverse	GTAGGGTCAAGTCGGGACATAA	
hnt	forward	TGACTTGACCAAGACGCAAG	627 bp
	reverse	GCTTTCTTGACCTCCTCACG	
***in situ* hybridization**			**Length**
Doc	forward	GAAGGCCAAATGGTCAGTGT	654 bp
	reverse	GTCGGGATGTTCGGAAACTA	
Doc (van der Zee et al., 2006)	forward	ATCCGCCGACTACTGCCTCTTCCT	518 bp (incl. 60 bp intron)*
	reverse	CTAACTGTTTCCGCTTCGCACTCG	
hnt	forward	TGACTTGACCAAGACGCAAG	627 bp
	reverse	GCTTTCTTGACCTCCTCACG	
twi	forward	GCTGATGGACCTGACCAACT	567 bp
	reverse	CTCCAATCACCCTCCATCC	
gsb	forward	GGCACCGTATTTCACTGGAT	630 bp
	reverse	GCCAGTTCTTCCCTGGTGTA	
zen2	forward	ATTACCATTCTCGGGGCTTT	818 bp
	reverse	GTGAGGTCAAGTTGGGTTGG	
dpp	forward	GTGGCATGTTGTTGGGGTAA	904 bp
	reverse	TGTGGTCTGGAATGGGGTAC	
zen1	forward	TCCCAATTTGAAAACCAAGC	688 bp
	reverse	CGTTCCACCCTTCCTGATAA	
pnr	forward	GTTCCATACAAGCGGTGGTG	1068 bp
	reverse	TCGCTTTTGATGGCACTTGT	
mid	forward	AGTTCAACGAATTGGGAACG	699 bp
	reverse	TCAGAAACAACTGCGACCTG	
Mmp2	forward	AAGTCCGGCTCGTCATTTC	1016 bp
	reverse	GAGTCGATTTCCGGTGAAAA	
iro	forward	AGTCCCACGTATCCCCTTTG	
	reverse	TCTTTCTCCTTGTCGTCGCT	
RT-qPCR			**Length** (gDNA/cDNA)
Doc	forward	GACCTGCAGACGGAGATGAT	3.784/109 bp
	reverse	CCAGGAAGAGGCAGTAGTCG	
dpp	forward	ATACGGAGCTTCACCCATGT	2.551/125 bp
	reverse	TTTATTTCGGCCGCTGTGAG	
hnt	forward	CAAGGGGTGCTCTTCATGC	3.031/133 bp
	reverse	TTTGGGTGCTTTGGTTCGTT	
Mmp2	forward	ACAATTTCCCCTTTGACGGC	2.648/153 bp
	reverse	GGGCCGCCACATTGAATAAA	
RpS3	forward	ACCTCGATACACCATAGCAAGC	186/186 bp
	reverse	ACCGTCGTATTCGTGAATTGAC	

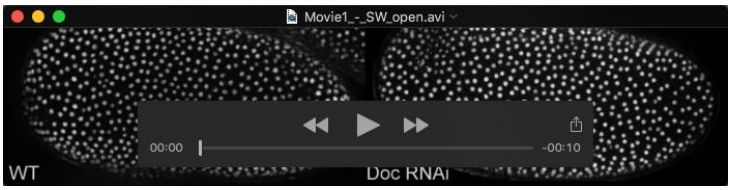

Movie 1. Serosal window closure fails after *Tc-Doc*^{RNAi}. Both embryos express nuclear-localized GFP (nGFP) ubiquitously and are shown in lateral aspect with anterior left and dorsal up. The movie shows early development of *Tribolium* including the last round of cell division in the uniform blastoderm followed by another round only in the germ rudiment (embryo and amnion). Left: wild type development showing the flattening of the posterior pole (primitive pit) followed by the formation of the posterior and later anterior amniotic folds. While the embryo invaginates, the border between the amnion and serosa forms the closing serosal window. Finally, the amnion and serosa detach from each other, releasing the embryo and the amnion into the yolk where they undergo germ band extension. For a schematic view of early development see main text Figure 8. Right: *Tc-Doc*^{RNAi} embryo showing normal cell division and invagination. However, closure of the serosal window slows down and finally stalls, tethering the head at a ventral position. Image stacks were acquired every 10 min at 24ºC and are shown as maximum intensity projections at each time point. The wild type and RNAi embryo are stage matched and shown at the same developmental rate, with elapsed time in hours and minutes indicated. See also main text Figure 4.

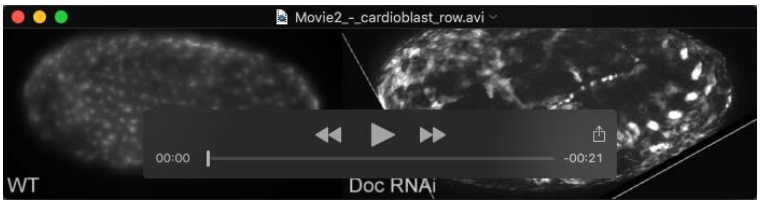

Movie 2. Serosal maintenance and cardioblast formation are unaffected by *Tc-Doc*^{RNAi}. Embryos are heterozygote crosses of enhancer trap lines that express EGFP in the serosa and embryonic domains including the cardioblast row, shown in lateral aspect with anterior left and dorsal up. The movie encompasses the late developmental stages of extraembryonic membrane rupture and withdrawal and embryonic dorsal closure. Left: wild type. Right: *Tc-Doc*^{RNAi} embryo with serosal window closure and posture defects, but with a persistent serosal tissue and wild type cardioblast row. Ultimately, dorsal closure fails in the *Tc-Doc*^{RNAi} embryo, and yolk can be seen spilling out over the embryo's head at the end of the movie. Image stacks were acquired every 10 min and are shown as maximum intensity projections at each time point. WT movie was taken at 30°C, while *Tc-Doc*^{RNAi} was taken at 24°C. See also Figure S6.

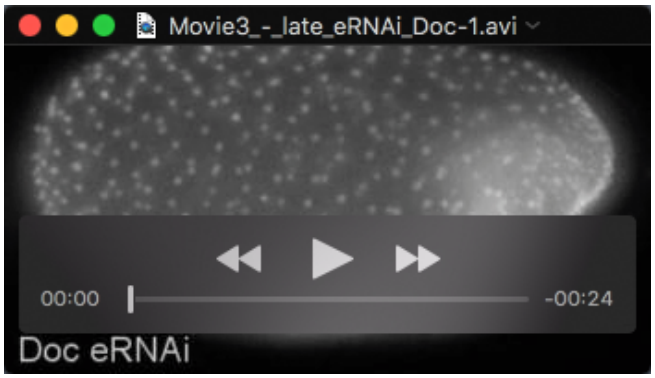

Movie 3. Later embryonic knockdown of *Tc-Doc* bypasses serosal window closure defects but still causes transient posture defects. The transgenic nuclear-GFP embryo was injected with dsRNA approximately 12h AEL and is shown in lateral aspect with anterior left and dorsal up, from serosal window closure through germ band retraction stages. Serosal window closure and anterior head extension are wild type, while posterior germ band extension is disturbed, characterized by a transient curling of the abdomen, but posture defects here are rescued during germ band retraction. Image stacks were acquired every 10 min at 30ºC and are shown as maximum intensity projections at each time point. See also main text Figure 4.

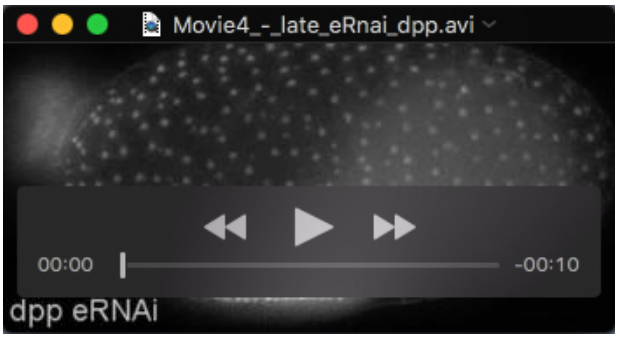

Movie 4. The *Tc-dpp*^{RNAi} phenotype after embryonic knockdown at approximately 12h AEL bypasses dorsal-ventral patterning defects but impairs morphogenesis. The transgenic nuclear-GFP embryo is shown in lateral aspect with anterior left and dorsal up, from serosal window closure through early germ band retraction stages. Serosal window closure is wild type, but the anterior amnion underneath the head shows defects, most likely due to an incomplete dissociation from the serosa. In addition, the posterior germ band extension is disturbed, characterized by a transient curling of the abdomen, similar to *Tc-Doc* embryonic RNAi. Image stacks were acquired every 10 min at 30ºC and are shown as maximum intensity projections at each time point.

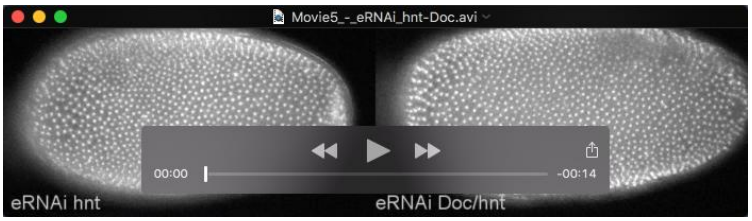

Movie 5. Loss of *Tc-hnt* or both *Tc-hnt* and *Tc-Doc* impairs serosal window closure. Embryonic RNAi against *Tc-hnt* (left) or both *Tc-hnt* and *Tc-Doc* simultaneously (right). The transgenic nuclear-GFP embryos are shown in lateral aspect with anterior left and dorsal up, from the uniform blastoderm through the extended germ band stages. Both embryos show a serosal window open phenotype similar to *Tc-Doc* RNAi alone (*cf.*, Movie 1). Note that the shape of the open serosal window was generally variable but did not differ between the three treatments. Image stacks were acquired every 10 min at 30ºC and are shown as maximum intensity projections at each time point. See also main text Figure 6.

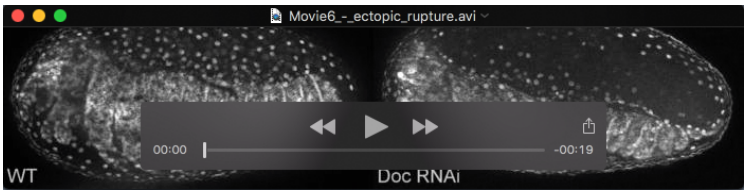

Movie 6. Extraembryonic membrane rupture defect after *Tc-Doc*^{RNAi}. The transgenic nuclear-GFP embryos are shown in lateral aspect with anterior left and dorsal up. Left: wild type rupture starts underneath the head, from where the EE membranes (only the serosa is clearly visible in the movies) pull back to the dorsal side to form the dorsal organ. Finally the back of the embryo closes during dorsal closure. Right: *Tc-Doc*^{RNAi} embryo showing ectopic rupture at the posterior pole resulting in a transient belt of extraembryonic tissue around the anterior abdomen. The formation of a functional dorsal organ fails, resulting in an incomplete extraembryonic cover over the yolk and finally lethal outflow of the yolk. Image stacks were acquired every 10 min at 30ºC and are shown as maximum intensity projections at each time point. See also main text Figure 7.

Movie 7. Dorsal closure defect after *Tc-Doc*^{RNAi}. The transgenic nuclear-GFP embryo is shown in dorsal aspect with anterior left. Extraembryonic membrane rupture and dorsal organ formation are morphologically wild type, but dorsal closure does not proceed in the posterior third of the embryo and finally the flanks of the embryo rip open again. Image stacks were acquired every 10 min at 24ºC and are shown as maximum intensity projections at each time point. See also main text Figure 7.